PMU-BASED PARAMETER IDENTIFICATION FOR THE SYNCHRONOUS GENERATOR DYNAMIC MODEL

by

CHIN-CHU TSAI

Presented to the Faculty of the Graduate School of

The University of Texas at Arlington in Partial Fulfillment

of the Requirements

for the Degree of

DOCTOR OF PHILOSOPHY

THE UNIVERSITY OF TEXAS AT ARLINGTON

December 2011

ACKNOWLEDGEMENTS

I would like to express my deep gratitude to my supervising professor, Dr. Wei-Jen Lee, for his guidance, encouragement, patience, and support throughout the development of this dissertation and my academic program. I feel so appreciative that Dr. Lee's financial support and professional guidance helped lead me to the end of my dream of pursuing a doctoral degree. I will be forever indebted to him for his unwavering moral support and sound advice during this period.

In addition, I'm so grateful to have this chance to convey my sincere acknowledge to my employer, Taipower Company, in Taiwan, for extending their sponsorship and support for these first two academic years, which made me not fear any difficulties from the start. A special note of appreciation is also extended to my previous and current bosses, Chin-Long Cheng and Hong-Wei Lan, who consistently provide me not only with expertise but also plentiful information on my research. Moreover, I wish to thank Dr. David A. Wetz, Dr. Rasool Kenarangui, Dr. Soontorn Oraintara, and Dr. William E. Dillon for their instruction, for serving on my dissertation committee, and for their valuable suggestions and review. I also want to express appreciation to all the members of the Energy Systems Research Center (ESRC), the University of Texas at Arlington, for all their valuable assistance, discussions, and enjoyable association. Apart from that, I would like to thank my colleagues at Taipower Inc. for their support and comments of this dissertation.

Last but not the least, I would like to dedicate my dissertation to all my family, especially to my wife, Shu-Chi Yang, for serving as my continued support and a constant source of inspiration for the tenure of my doctoral degree. I am full of thankfulness to them for their love, encouragement, and endless support.

November 2, 2011

ABSTRACT

PMU-BASED PARAMETER IDENTIFICATION FOR THE SYNCHRONOUS GENERATOR DYNAMIC MODEL

Chin-Chu Tsai, PhD

The University of Texas at Arlington, 2011

Supervising Professor: Wei-Jen Lee

Power systems have become more complex and are found to be consistently operating closer to their stability limits under the deregulated environment. Power system dynamic simulation, which provides significant insight into the dynamic characteristics of system, is one of the most important tools for both planning and operation engineers. Since it heavily relies on the simulation result to make decisions related to operation strategies, grid expansion plain, facility maintenances schedules, an accurate simulation result can avoid unnecessary facility investment and improve the security of the system operation. However, the simulation result is affected by the model and parameters of the equipment. Since most models are provided by the manufacturer and derived through rigorous verification; it is reasonable to assume that model be trustworthy. However, there are many tunable or user definable parameters in the model. Assigning inaccurate parameters become the major source that causes the mismatch between the simulation results and actual system response. However, a large power system is composed of millions of component and many of them are inter-correlated, the parameter identification becomes very difficult.

This dissertation proposed a hybrid dynamic simulation strategy for parameter identification based on measurement data of phasor measurement unit (PMU). It efficiently makes a boundary on the measurement point of PMU to overcome the uncertainty of the external system elements which makes the proposed task manageable.

To improve the computational efficiency, this dissertation also proposes a key parameter screening process based on trajectory sensitivity to identify the most significant parameters. A high efficiency global optimization algorithm called cooperative simultaneous perturbation stochastic approximation and particle swarm optimization (SPSA-PSO) is proposed to solve the parameter identification problem. The effectiveness and feasibility of the proposed method and process were demonstrated by a new installed generator unit in Electric Reliability Council of Texas (ERCOT) system.

TABLE OF CONTENTS

LIST OF ILLUSTRATIONS

Figure Page

LIST OF TABLES

CHAPTER 1

INTRODUCTION

1.1 Research Background

In recent years, the United States electric utility industry entered the phase of restructuring and deregulation. The traditional vertically integrated electric utility structure has been replaced by a horizontal structure with unbundled generation, transmission, and distribution companies in nearly half of the states [1]. Deregulation results in a more intensive use of the transmission network which pushes the electrical power system closer to the stability limit. Thus, the power system stability problem is more important and serious than ever.

Power system dynamic simulation is widely applied to the study of the power system stability problem. It is an important tool to provide an insightful inspection of system dynamic characteristics after a disturbance. Therefore, power system design, planning, and operation engineers make decisions based on the results of dynamic simulations. The accuracy of dynamic simulation directly impacts the correctness of the engineers' and companies' decisions.

Dynamic simulation results heavily depend on the accurate parameters of the system components such as generators, exciters, governors, power system stabilizers, and loads. Studies conducted by the Northeast Power Coordinating Council also showed that, "in general, in stability analysis it is more important to use accurate machine data than elaborated machine models" [2].

1.2 Power System Parameter Identification

Dynamic modeling and studies which reveal the dynamic characteristic of a power system play more critical roles in the planning and operation of power systems. The dynamic

simulation results are highly dependent on the parameters of the system components such as generators, exciters, governors, and loads. Unfortunately, many parameters in the system are not accurate due to the following reasons:

- The dynamic parameters available to the Independent System Operator (ISO) are usually from generator owners. They collected the parameters from the manufacture data and/or on-site testing before the first operation. Some parameters may drift over a long period of operation or the replacement of components. In addition, it is very difficult to ask generator owners to check and update the parameters by performing frequent on-site tests.
- Some parameters obtained from the manufacture data are a range of values and they can be re-adjusted during practical operation. The mean value sometimes is sent to the ISO from the generator owners.
- Some parameters are not available from manufacture data or on-site testing. The ISO has to replace them by some typical value or by using the same value from the other generation with the same/similar dynamic model.

It is common to see some mismatches between dynamic simulation results and the actual system response because of inadequate dynamic parameters. Too pessimistic simulation results will lead to conservative operation decision of transfer limits such as available transfer capacity (ATC) and total transfer capacity (TTC) in the system, and then result in additional congestion cost in the power market and reduce asset utilization of the transmission network. In contrast, too optimistic simulation results may also lead to over-estimate the transfer capacity and gave the operators the false sense of security of the system. Moreover, an unnecessary facility investment can be avoided when the simulation results are accurate.

The impact of such over-optimistic estimations may cause a power system from a minor contingency event to cascading blackouts in a worst case scenario. A large blackout (about

30GW load loss) occurred in the Western Systems Coordinating Council (WSCC) system on August 10, 1996 [3]. The dynamic simulation results based on the standard WSCC dynamic database illustrate no stability problem in the system which is in direct contradiction to the actual system disturbance response as shown in Figure 1.1 and Figure 1.2. After that, WSCC established the Governor Modeling Task Force and the Load Modeling Task Force to address this issue. They modified some dynamic models such as exciters, governors and loads. A very good agreement was achieved between simulation results using the modified models and recordings, as shown in Figure 1.3 and Figure 1.4.

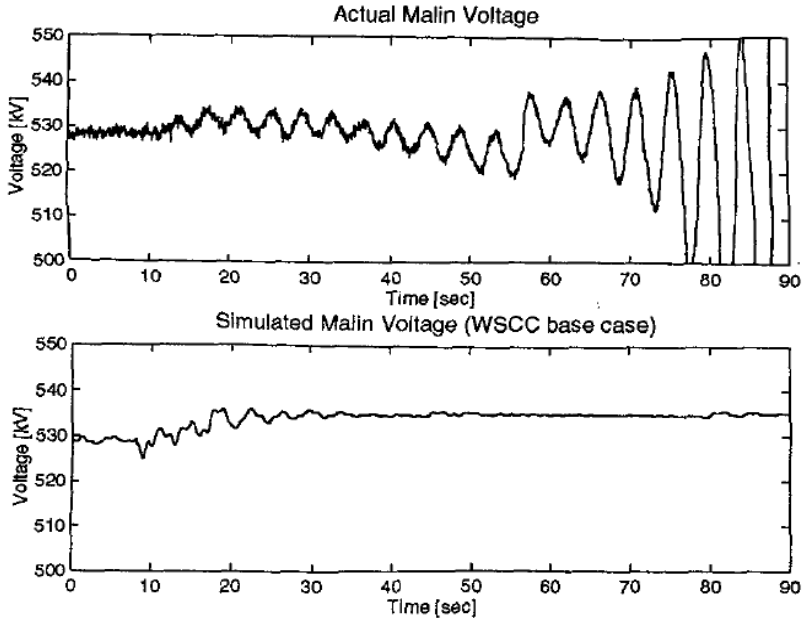

Figure 1.1 Voltage - Recorded and the Simulated Using the Standard Models (WSCC, 1996)

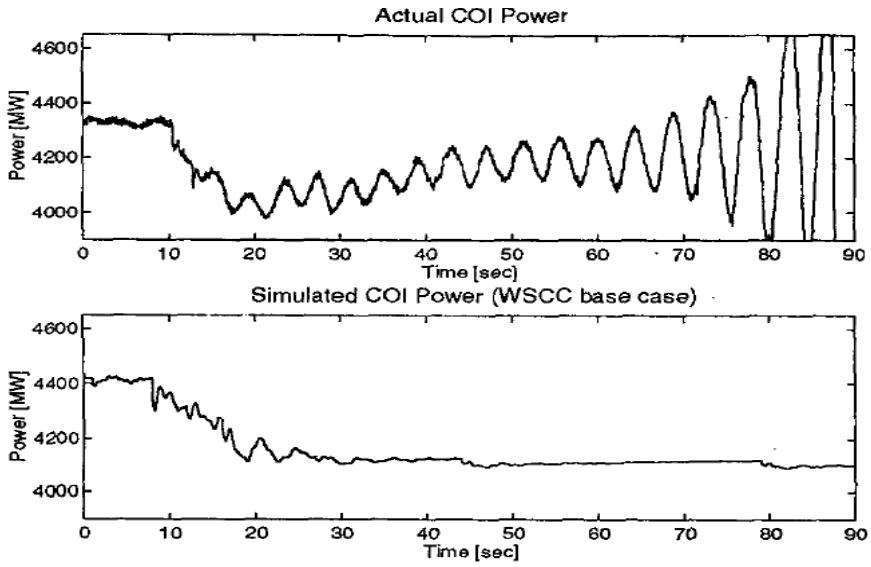

Figure 1.2 Active Power - Recorded and the Simulated Using the Standard Models (WSCC, 1996)

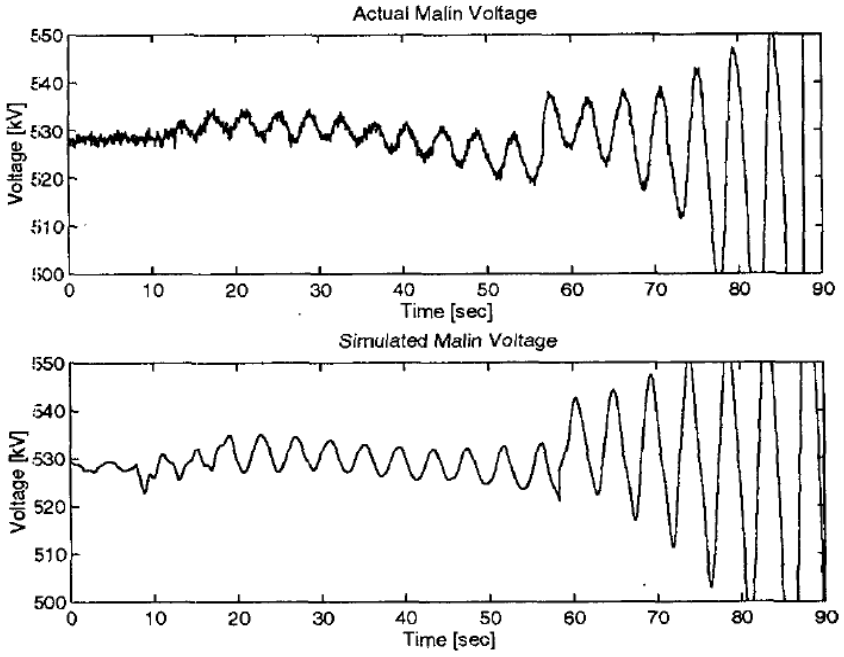

Figure 1.3 Voltage - Recorded and the Simulated Using the Modified Models (WSCC, 1996)

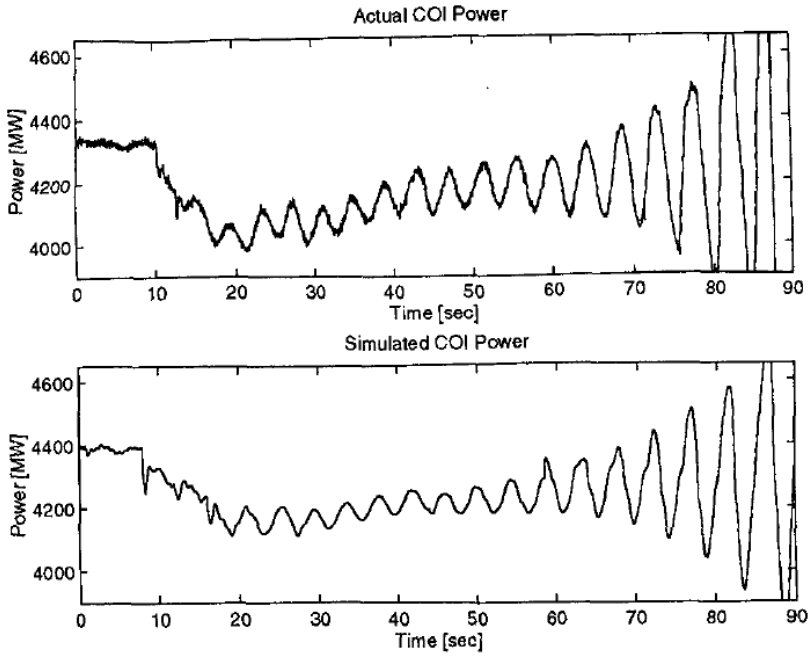

Figure 1.4 Active Power - Recorded and the Simulated Using the Modified Models (WSCC, 1996)

Eight years later, on June 14, 2004, a major disturbance resulted in approximately 1000MW load loss in the Western Electricity Coordinating Council (WECC, the successor of WSCC) [4]. As usual, WECC simulated the dynamic events and compared the simulation results with the recorded data. The initial simulation successfully reproduced the system frequency performance. However, the initial simulation failed to replicate the voltage profile in some areas. As a result, WECC had to re-start the model validation work again. The process lasted for more than one year and most of the work was manually and jointly performed by several utilities in WECC. Finally, the simulation results turned out to be closer to the recordings after some parameters were fine-tuned. The lessons learned in the WECC model validation effort can be summarized as follows:

- Maintenance of the dynamic models and parameters is a long-term and on-going effort. The planners and operators of the system need to study and update them on a continual basis.
- Maintenance of the dynamic models and parameters is a local problem. The mismatch between the simulation and disturbance event records usually can be fixed through the adjustment on the models and parameters of the local devices such as generators and their associated control apparatuses.
- Since manual adjustment is time consuming and it is difficult to obtain an optimal solution, it is necessary to develop an automated procedure for the parameter estimation.

For the above reasons, this dissertation is dedicated to develop an on-line automatic parameter identification process for generator units.

1.3 The Proposed Implementation Method

The proposed dynamic model parameter identification scheme in this dissertation is an on-line PMUs-based application. The necessary PMU measurements for this application are merely voltage, angle/frequency, real power, and reactive power – (V, δ / f , P, Q). The internal information of the generator, such as field voltage and rotor speed, is not needed for this proposed method. Therefore, this proposed approach offers a feasible solution for ISO's to independently identify the model's parameters.

It is a good indication that the simulation model or its parameters could be wrong or inadequate, if the simulation results have significant mismatches with actual system responses. A further fine tuning process for a model's parameters is necessary. Since it is difficult, if not impossible, to obtain complete pre-fault information, a system wide detail simulation is impractical. The hybrid dynamic simulations can effectively equivalent the outside system which uses PMU measurement points as a boundary. This equivalent approach not only simplified the

tedious manual procedures to rebuild the pre-disturbance system condition but also ruled out the simulation mismatches which are caused by outside systems and reduce the computational burden.

After system reduction has been done by the hybrid dynamic simulation, the trajectory sensitivity analysis is used to screen out the parameters regarded as key parameters to further improve the efficiency of the proposed algorithm. Since only key parameters have significant impact on the system response and will be fine tuned, the number of calibrating parameters can be deducted and the computation burden can be effectively reduced without scarifying the correctness of the model's behavior. Finally, a new proposed optimization algorithm, cooperative SPSA-PSO, will take place to identify a set of parameters to minimize the mismatch between the simulation result and field measured data. This proposed algorithm preserves SPSA's fast converge ability and PSO's global searching ability. Therefore, an acceptable solution can be achieved in finite iterations.

1.4 Assumptions and Contributions

1.4.1 Assumptions

The proposed method focuses on parameter verification for the governor, exciter, and power system stabilizer models used in the power system simulation. The dynamic model itself is assumed to be correct. This assumption is reasonable since the model was developed by the manufacturer and gone through both factory and on-site testing prior to the commercial operation.

Some electrical quantities are very sensitive to the dynamic parameters. For example, E_{fd} (exciter field voltage) is very sensitive to exciter parameters and can be used to identify the accuracy of these parameters. However, it is not practical to capture the value of E_{fd} during routine operation. In addition, it is usually hard for an ISO to request Independent Power Producers (IPP) to provide internal operation condition of the generators after deregulation.

Therefore, only the on-line PMU measurement data on the grid side and at generator-grid interface are utilized for dynamic parameter identification in the proposed method.

1.4.2 Contributions

The proposed SPSA-PSO cooperative algorithm provides the right balance and trade-off between convergence speed and global searching ability. This algorithm is not dependent on the initial guess and exhibits superior performance in terms of simulation time. The proposed method improves the solution accuracy and computation time of the PSO algorithm which has been identified by many researchers in power system optimization [5].

The proposed parameter identification process is a model independent approach. Although this dissertation focuses on dynamic parameter estimation of exciters, PSS, and governors, the method can easily be extended to dynamic parameter estimation of other device models in power systems such as dynamic load models. A commercially available power system simulation software, PSS/E, is utilized as the simulation engine in the proposed parameter identification process so that the proposed method is applicable to and works well on large-scale systems.

A system equivalent approach, hybrid dynamic simulation, has successfully adopted and modified in this dissertation for solving parameter identification problem and the detail implementation issues have been addressed. In addition, there are more than ten parameters in most exciter, power system stabilizer, and governor models. It will pose significant computation burden if one has to identify all of them. Based upon their impact on the system response, this dissertation analyzes and categorizes them into different groups. Those parameters which are adjustable and have a great impact on the dynamic simulation are defined as key parameters. Only the key parameters are needed to be incorporated in the estimation process which decreases the complexity and computation burden. Meanwhile, the correlation of parameters is

analyzed to assist the interpretation of the calibrated results and it will also benefit the model/parameter estimation work in the future.

1.5 Synopsis of Chapters

The organizational structure associated with this dissertation is as follows:

Chapter 1 introduces the general background of the power system dynamic parameter identification, illustrates the importance, motivation, and objective of this dissertation.

Chapter 2 reviews the historical research approaches, techniques, and the progress of the regulations which are relate to generator model validation or parameter identification.

Chapter 3 describes an impotent system equivalent methodology, hybrid dynamic simulation method, in detail. This chapter focuses on comparison and discussion of the performance of different approaches when it applies on generator parameter identification.

Chapter 4 presents the process associated with key parameters screening and parameter correlation analysis. The key parameters can be identified by trajectory sensitivity analysis developed in PSS/E dynamic simulation. The Singular Value Decomposition (SVD) method also developed to carry out the relationship among key parameters and improve the resolution of estimated results.

Chapters 5 introduce the proposed SPSA-PSO cooperative algorithm in detail. The advantage and disadvantage of both SPSA and PSO algorithms also be discussed.

Chapter 6 uses a new installed generator in ERCOT system as test case to demonstrate the validity of parameter identification process and the distinct advantages of the proposed optimization method. The detail application issues also address in this chapter. Moreover, the results show that a good agreement between the recorded information and the simulation results which derived with modified parameters obtained from the proposed identification process.

Chapter 7 presents the conclusions and recommendations drawn from the research associated with this dissertation and discusses the opportunities for further research.

CHAPTER 2

LITERATURE REVIEW

2.1 Survey of Parameter Estimation Approaches

Since the late 60's, many studies has been conducted to determine the parameters of the synchronous generator unit. The modern techniques used can be classified into two typical approaches: field test, as in examples [6], [7], [8], [9] and on-line measurements, as in examples [10], [11], [12], [13]. Field tests are a good means to gain direct insight into dynamic parameters. They are usually preformed to establish the initial models and parameters before the new device is commissioned. However, parameters may be drifted or adjusted after continued operation or maintenance. Frequent field tests which require shutting down a unit several days for doing the test would be either impractical or even impossible due to the potential damage and high costs. In order to overcome the shortcomings of the field test method, online based identification methods have drawn attention to this application in recent years. The following literature review, hence, is based on online-based identification methods used to classify the different approaches according to different type of generator model, measurement data, and identification algorithm respectively.

According to the difference types of identification models, the methods can be roughly divided into two categories. In the first category, a known structure is assumed for the generator units (as the field test methods), and the unit's parameters are estimated from online measurements. The second category treats units' models as black-boxes to represent the behavior of input/output data. In the black-box modeling, the structure of the model is not assumed to be known prior to the test. The only concern is to map the input data set with the output data set. Many different approaches, such as identification of nonlinear systems, like

generator, have theoretically been attempted using Nonlinear Least Squares, Wiener series [14], volterra series [15], Wavelet Nonlinear ARX Network [16], and Neural networks [17]. These black-box models can be used for system analysis and controller design, especially when designing a power system stabilizer (PSS) [15].

Many researchers have proposed algorithms to solve the parameter estimation problems using online measurements. One of the methods [18] employed was the recursive maximum likelihood (RML) estimation technique for the identification of an armature circuit parameter. The field winding and some damper parameters are estimated using output error method (OEM) techniques. Their objective function is to minimize errors by using the iterative Gauss Newton method, and the data set required for estimation consists of field side current, terminal voltages, and currents. Reference [11] required currents, voltages, and the generator speed to perform the proposed identification process. The estimation of generator's parameters is decoupled offering a more robust estimation algorithm. In order to achieve this robustness with respect to the initial parameter guess, the Differential Algebraic Equations which model the generator are replaced by a constrained minimization problem that overcomes singular problems of the algebraic equations. Reference [10] proposed a procedure for identifying an excitation model through information from online measurements, voltage regulator and field voltage, and a plant transient recorder system. The parameter fitting algorithm is formed as an optimization problem and solved by the Newton method. A conjugate type stochastic approximation (SA) algorithm is proposed in [19] to deduce wind turbine parameters from the disturbance measurements of active and reactive powers. The reported approaches have a common point that uses the generator unit's field measurement signals during dynamic events to gain direct insight into the dynamic characteristic. Although the results shown that the online measurements approach can precisely estimate most of the parameters, it is difficult for an ISO

to obtain the details and internally recorded data of a generator from the Independent Power Producers (IPPs).

Another alternative approach for dynamic parameter estimation is the PMUs-based method. PMU devices and PMU-equipped numerical relays can provide time-synchronized data necessary for the parameter identification with good resolution and high sampling rate. Moreover, the Energy Management System (EMS) can provide the steady-state pre-disturbance data needed for parameter identification. Therefore, the PMUs-based approach becomes a promising solution for the parameter identification problems. However, little research has been carried out regarding this problem since this is a relative new technologies. Reference [13] proposed a method that used whole system simulation with a curve fitting approach to estimate parameters. However, due to whole system simulation, the performance of the algorithm is slow, and the accuracy of estimated result is not guaranteed. Although [19] successfully developed a system reduction technique that improves computational efficiency and the estimation precision, the detailed application issues and performance of the optimization algorithm are not well defined. In [20], the authors employed an extended Kalman filter to calibrate the parameters of the dynamic models for a power system. Using the data from the PMU following a fault, the parameters converged to the true value by a prediction-correction process. However, the noise effect is not studied in this paper. Theoretically, the extended Kalman filter is not an optimal estimator since both the measurement and the state transition model are non-linear. Therefore, the estimation results are less accurate. The purpose of this dissertation is dedicated to develop a high efficiency algorithm and a detailed application scheme for solving PMUs-based dynamic model parameter identification problems. A brief review of the PMU technologies and its potential applications is provided in the following section.

2.2 PMU Applications

A phasor is a complex number that represents both the magnitude and phase angle of the sinusoidal waves found in electricity. Phasor measurements that PMU devices sample at the same time are called "synchrophasors". In typical applications, PMUs are sampled from widely dispersed locations in the power system network and synchronized from the common time stamp of a Global Positioning System (GPS) radio clock. Synchrophasor technology provides a tool for system operators and planners to measure time-stamped voltages and currents at diverse locations in a power system. By utilizing PMUs, the reliability and stability in a given power system are expected to improve. Figure 2.1 shows the PMUs installation map in North American in early 2011.

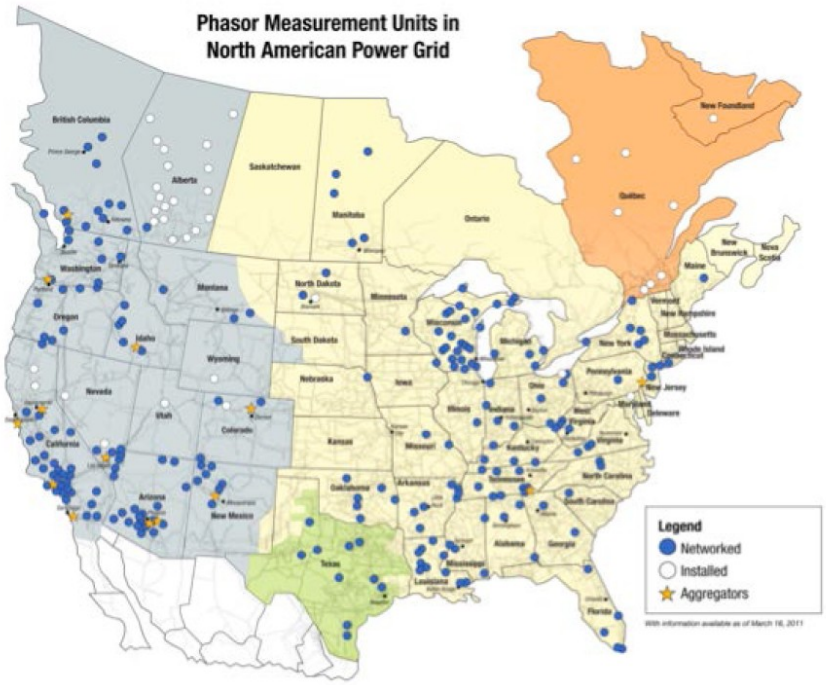

Figure 2.1 PMU Locations in Early 2011 [21]

In 2007, the organization of U.S Department of Energy (DOE) and the North American Electric Reliability Corporation (NERC), along with involved electric utility companies and other

organizations, formed the North American SynchroPhasor Initiative (NASPI) [21]. The goal of NASPI is to improve power system reliability through PMUs measurement, monitoring and control. This will be archived by installing PMUs data measurement infrastructure for the interconnected North American electric power system and by developing associated analysis and monitoring tools for better planning and operation, and improved reliability. With funding from both The American Recovery and Reinvestment Act of 2009 (Recovery Act), several smart investment grant and demonstration projects have been awarded to advance the synchrophsor technology. The Recovery Act provided significant funding for smart grid technology, with $4.5 billion of Federal funding allocated to projects that involve significant industry cost share. Two major categories of projects were included as parts of the Recovery Act: Smart Grid Investment Grants (SGIG) and Smart Grid Demonstration Projects (SGDP). Specifically, $3.4 billion of Federal funding was allocated to SGIG, which were intended to be near-term projects that required a minimum of 50% cost match from the industry [22]. These projects were organizes into six categories one of which involve synchrophasor technology were associated with the electric transmission systems category. Companies that submitted proposals which were selected for award include:

- American Transmission Company, LLC
- Duke Energy Carolinas, LLC
- Entergy Services, Inc
- Midwest Energy, Inc
- Midwest ISO, Inc
- ISO New England, Inc
- New York ISO, Inc
- PJM Interconnection, LLC
- Western Electricity Coordinating Council

And, the projects which involved the synchrophasor applications include:

- Wide-Area Visualization and Monitoring
- Angle and Frequency Monitoring
- Interarea Oscillation Detection & Analysis
- Proximity to Voltage Collapse
- State Estimation
- Dynamic Model Validation
- Fast Frequency Regulation

Although the above applications are from the view of ISO, The PMUs-based applications also benefit generator owners. PMUs are able to continuously record several different signals which are the requirements of ancillary services like spinning reserve, frequency control and voltage control. Once the infrastructure is permanently installed at the power plant, the online tests such as voltage step-change can be easily applied and recorded.

Since this dissertation is focused on dynamic model parameter identification, only the PMU's application of dynamic parameter validation issues is addressed. Reference [23] presents an PMU's recorded voltage and a frequency injection approach for generator model validation based on the PMU measurements taken at the point of interconnection. The approach is applied for the Dallas, Jone Day, and the Grand Coulee powerhouse in WECC system. Based on this method, [24] named this approach as "hybrid dynamic simulation" and implemented in a commercial power analysis software, PSLF/PSDS. Additionally, a small system case has been demonstrated to extend this approach to a system-wide usage. Two application examples in [24] on generator and load model validation are presented to show the validity of this methodology. Therefore, model validation and parameter identification could be a feasible application of PMU.

2.3 Relatively Regulation

Model validation and parameter identification are not only an important issue for power engineer, but also the requirement of new regulatory standards for measurement and verification of dynamic models for generators and their control systems. In order to ensure that generator models accurately reflect the generator's capabilities and operating characteristics, the NERC has addressed verification of generator dynamic models in its now retired Planning Standards, and the NERC is currently developing Reliability Standards containing mandatory and enforceable requirements for verification of these generator dynamic models, as in [25].

As a result of the August 14th, 2003 northeast blackout and associated investigation, the NERC Board of Trustees in February 2004 approved 14 recommendations to address the shortcomings that contributed to the blackout [25]. One of these recommendations was to direct the NERC Regions to implement processes for validating power system models and data including generator dynamic models. This same recommendation was repeated in the final report of the US Canada Power System Outage Task Force [26]. Subsets of the Planning Standards were converted to "Version 0 Reliability Standards." The Version 0 Reliability Standards became effective in April 2005. However, compliance with these standards was voluntary.

Planning Standards Section IIB is the base line for the current Reliability Standard drafting efforts regarding generator dynamic models by the NERC Generation Verification. Regarding the verification of generator excitation model verification, the most relevant Measurement (M6) states "Generation equipment owners shall verify the dynamic model data for excitation systems (including power system stabilizers and other devices, if applicable) at least every five years". Designed data for new or refurbished excitation systems shall be

provided at least one year prior to the in-service date with updated data provided once the unit is in service, as in [25].

The current Reliability Standards related to generator model verification are:

- MOD-026-1 — Verification of Models and Data for Generator Excitation System Functions
- MOD-027-1 — Verification of Generator Unit Frequency Response
- PRC-002-1 —Define Regional Disturbance Monitoring and Reporting Requirements

Standards MOD-026 [27] and MOD-027 [28] are currently under development and focus on the validation of the dynamic simulation models. Both standards included the following common draft Requirements:

1) The Regional Reliability Organization (RRO) was responsible for the development and maintenance of the applicable dynamic model verification procedures. The RRO procedures were required to include generating unit exemption criteria, acceptable dynamic modeling verification methods with verification periodicity and scheduling, and an additional list of supplementary information. This list included manufacturer and type of associated equipment, the verified model and model data, the verified response data, and the method of verification used.

2) The aforementioned generator owner was given the responsibility of following the RRO procedures MOD-026-1 and MOD-027-1.

From a high-level viewpoint, the goal of the model test was to determine whether it was feasible to implement the current draft versions of the MOD-026 -1 and 027-1 Reliability Standards. Moreover, The Standard Drafting Team felt that the standard should be written based on applicable techniques. The techniques which are under development or in limited use but could become common in the future if they are found to still fit well within the Reliability Standard Requirements. Therefore, the current draft of the standard states “what is required”

instead of stating “how to accomplish the required” [25]. For example, the traditional field testing, such as open step voltage tests, could be a possible method. Any technique that adequately demonstrates correlation between the responses predicted by the excitation system models to voltage variations in comparison to actual equipment performance becomes an acceptable way to verify excitation system models. In addition, using recorded power system quantities which were captured during natural system disturbances that result in an excitation system response, the predicted model response can be compared to the actual equipment response by capturing key electrical parameters associated with the excitation system response. The proposed model identification procedure verified the simulation with PMUs measurements is adequate to meet the requirements of the new standards.

Moreover, NERC Standards PRC-002 [29] require the installation of disturbance monitoring equipment (DME). The RRO should develop a plan with the criteria and requirements for the installation of such instrumentation, as well as the technical requirements associated with the signals to be recorded. Generator owners are required to comply with the requirements posed by the RRO deployment plan, in which case instrumentation would have to be installed at selected power plants and/or substations. Reference [30] discusses that the characteristics of the instrumentation which are usually applied to record commissioning tests, and tests associated with the dynamic model validation are a close match to the requirements derived from the PRC-002 Standard. Significant savings could be achieved if the instrumentation installed to comply with the PRC-002 Standard could also provide the necessary data for the dynamic model validation required under Standards MOD-026 and MOD-027. Generator owners in particular should be aware of the potential savings that could be achieved by combining all of the data recording necessary to comply with the disturbance monitoring (PRC-002) and model validation (MOD-026 and MOD-027) Standards. Like the main

ideal of this dissertation, PMU based model identification, can satisfy the requirements of both monitoring and model validation standards at the same time.

2.4 Review Conclusions

Dynamic simulations are applied in the assessment of the adequacy, security, and reliability of the power systems. In particular, dynamic stability simulations are concerned with the ability of synchronous generators to stay in synchronism with the power grid following different disturbances, which usually involve faults in the system and the subsequent response of the protection schemes to clear these faults.

NERC standards, once approved, will establish a maximum time period between model validation tests. It is expected that the Standards MOD-026 and MOD-027 would impose a certain periodicity for the revalidation of the models. In other words, compliance with these Standards would become a continuous mandatory effort.

PMUs, relatively inexpensive monitoring devices, are able to continuously record several different signals. They are becoming widely available and might become standard equipment installed at large power systems to meet the demands of the increasing requirements for monitoring of system stability and security. The approaches of using data associated with online operation of synchronous generators for the validation of dynamic simulation models is not new and significant research effort has been reported in research and literature over past several decades. However, the research devoted on the PMUs based model identification problem is not extensive, by any means. Thus, further research on the application of PMUs based model identification approaches should be supported.

CHAPTER 3

HYBRID DYNAMIC SIMULATION

Since the generator is attached to the system and it is not clear how uncertainties derived from the power system side could affect the estimation process. The traditional simulation system reduction method is able to use equivalent models for the external system to remedy the uncertain effect that comes from the system. Since an equivalent model is an approximate of the physical system, simulation error is inevitable. Recently, a hybrid dynamic simulation concept has been reported for the purpose of model validation [23] [24]. This method allows for the dynamic simulation of a subsystem with measured signals injected at its boundary without introducing errors caused by an external systems model. This method employs PMU measurements, which accurately record the system behavior, at the boundary to precisely represent the response of external system in the simulation. This dissertation modifies the original concept of hybrid dynamic simulation and applies in the generator parameter identification and incorporated the idea of the hybrid simulation algorithm into commercial power system simulation software (PSS/E) by using the time-series measures records for the desired function.

3.1 Introduction of Hybrid simulation

The dynamic behavior of a power system can be represented by a set of differential algebraic equations as shown in (3.1).

$$\begin{cases} \dfrac{dx}{dt} = f(x, y, \lambda, u) \\ 0 = g(x, y, \lambda, u) \end{cases} \tag{3.1}$$

where $x = \{x_1, \cdots$ denotes the dynamic state variables, such as the rotor angle and the rotor speed etc, and $y = \{y_1, \cdots$ denotes the algebraic variables, such as the bus voltage and the phase angle; λ denotes the parameters and u denotes the controls. As power system simulation software is applied to solve (3.1), the results of each computation step are available to the user to proceed with the next step; therefore, the evolution of the system dynamics with respect to time can be derived. In addition, when the synchronized record data is available, hybrid dynamic simulation becomes possible. The hybrid dynamic differential algebraic equation can be described as follows:

$$\begin{cases} \dfrac{dx}{dt} = f(x_1, y_1, \lambda, u, x_2, y_2) \\ 0 = g(x_1, y_1, \lambda, u, x_2, y_2) \end{cases} \tag{3.2}$$

The dynamic state variables x and the algebraic variables y in (3.1) are classified into two subsets, $\{x_1, y_1\}$ and $\{x_2, y_2\}$. The subset $\{x_1, y_1\}$ includes all the states that could be derived from a step by step breakdown of digital simulations, and the subset $\{x_2, y_2\}$ includes all the variables that could be obtained from the PMUs. The basic idea of the hybrid dynamic simulation can be illustrated by Figure 3.1. If the Phasor Measurement Unit (PMU) is installed at the boundary of the subsystem, then the whole system can be merely represented by the subsystem using the information from the PMUs. Therefore, only the models and parameters of the components in the subsystem and the actual measurements from the boundary of the subsystem are needed for the simulation. Through this approach, the simulation validation work can be reduced into a much smaller region.

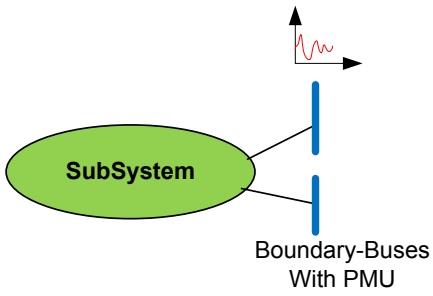

Figure 3.1 System Reduction Employing PMU Measurements

Hybrid dynamic simulation provides an entry for PMU measurements to integrate with the traditional dynamic simulation. Applications of such hybrid simulation include [31]:

- *System Scenario "Playback"*

  Power systems have experienced some severe failures in this decade. Post-event analyses are important to figure out the problems of system and prevent the same failure from occurring. Hybrid simulation employing measurements can assist in this way, gaining better understanding of system behaviors and identifying the causes of failure.

- *Software Validation.*

  With validated models and measurement records, software simulated results can be compared with records to evaluate the simulation software.

- *State Estimation.*

  PMUs have been installed at many important locations nationwide and have recorded quality measurements for system analysis, monitoring and control. However, still numerous signals are not measured by PMUs. In this case, hybrid simulation can use available measurements to generate those unmeasured signals. This method can be used offline with archived historical data, or real-time with online measurements if the simulation is fast enough.

- *Model Validation.*

  Comparison between measurements and simulation results have been employed to validate models used for simulation, as in [13]. However, a real power system, e.g. ERCOT system has hundreds of models, each of which may contribute to the error between measurements and simulation. Therefore, it is very difficult to locate the real modeling problem which causes the mismatches in a large system. In hybrid dynamic simulation, such a comparison can be done in a reduced subsystem with measured signals which are injected as boundary conditions, as shown in Figure 3.1. The measured and simulated power flows can be compared and the mismatch can indicate modeling problems inside the subsystem. This generator model validation method is been applying to validating some WECC models [23].

In power systems, four quantities are usually associated with the system status: voltage, angle/frequency, real power and reactive power – (V, δ / f , P, Q). Ideally, if any two of them are known, one can solve for the other two through simulation. Hence, hybrid dynamic simulation according to their implementation method can be classified into two approaches. The first one, voltage-injection, forces the voltage and angle as recorded data at the measurement points [31] [23] [24]; the other, Load-injection, matches the real and reactive power at the measurement points [19]. The idea of the two methods is explained in the following section.

3.2 Voltage injection method

Currently, a phase shift method [31], classified as a voltage-injection approach, is proposed for model validation and implemented for parameter identification. Phase shift method is an indirect implementation method of hybrid simulation as shown in Figure 3.2. In order to retain the response of boundary bus, a dynamic device needs to be added at the boundary bus to create the entry point for measurements.

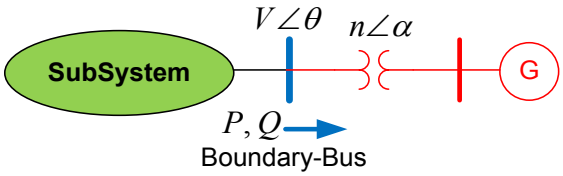

Figure 3.2 Phase Shift Method of Hybrid Dynamic Simulation

In Figure 3.2, the boundary bus is the location where voltage magnitude (V), angle (θ), real (*P*) and reactive (*Q*) powers are measured by PMU. The objective is to enforce both the measured voltage and the angle records at the boundary bus during the simulation. As a result, an artificial generator and an ideal transformer are added at the boundary bus. The model of the generator is a classical generator model with zero internal reactance, very high inertia constant, and zero damping rations. The transformer is a near zero impedance ideal transformer. The initial conditions for the added generator and transformer are determined as follows:

- The voltage setting for the generator is 1 pu.
- The initial power output of the generator is the initial load flow on the transmission line where the measurement point is located.
- The initial turn ratio (n) of the transformer is the initial recorded bus voltage (V).
- The initial phase shift (α) of the transformer is the initial recorded bus voltage angle (θ).

By adjusting the turn ratio and phase shifter of ideal transformer at each simulation step, the voltage and the angle at the boundary bus can be matched to the measurements. A demonstration case is built for testing the performance of hybrid dynamic simulation. The mismatch between simulation results and measurement data of real power, reactive power, voltage, and angle are shown in Figure 3.3 (a), (b) and Figure 3.4 (a), (b) respectively. The diagram with the legend “Rec” is the simulation result of the whole system and is assumed as the recorded data at the PMU boundary bus. Then, injecting this recorded data at PMU boundary bus and running the reduced system, the hybrid simulation results are shown by

legend “Sim.” The results proved that the phase shift method can reliably present the system dynamic response for model variation purposes. However, the simulation mismatch can be noted at Figure 3.3, the effect of which will distort the results for parameter identification process.

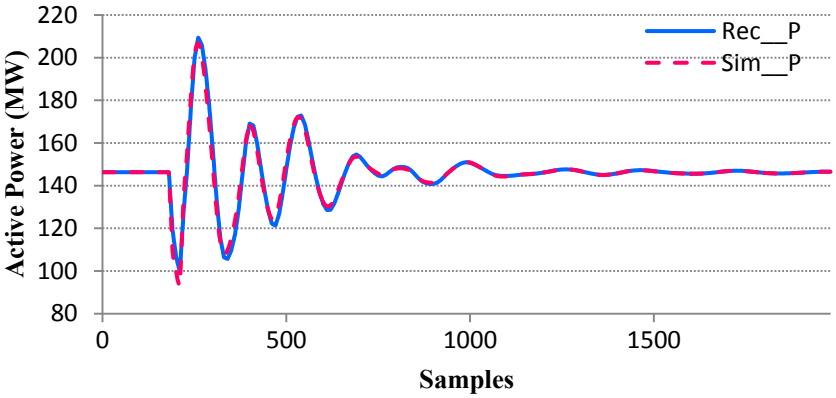

(a)

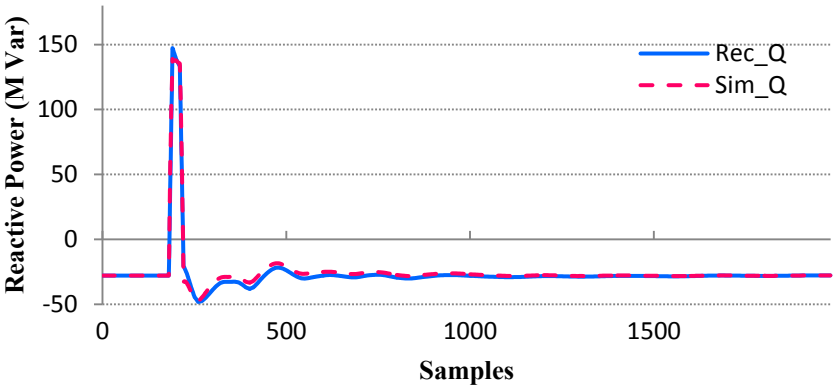

(b)

Figure 3.3 Comparison of Simulation Result and Record Data (a) Real Power (b) Reactive power

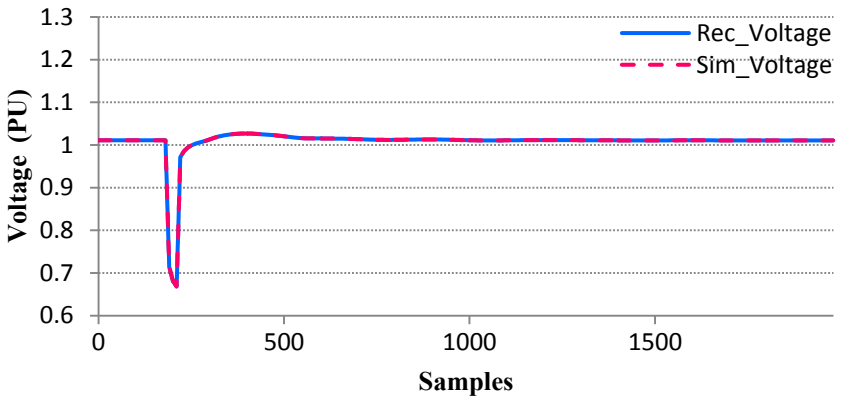

(a)

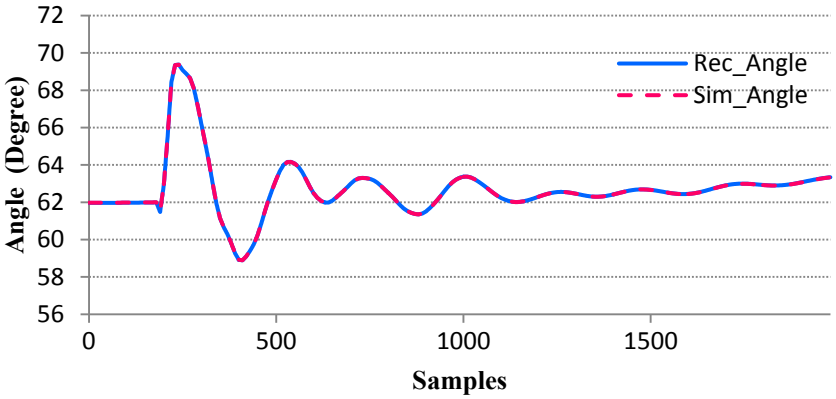

(b)

Figure 3.4 Comparison of Simulation Result and Record Data (a) Voltage (b) Angle

The mismatches of simulation results are shown in Figure 3.5. These inherent mismatches are caused by the added ideal generator and transformer is not accepted by analysis software. Therefore, for parameter identification problem, the simulation mismatching issue should be addressed and the further discussion will be presented in chapter 5.

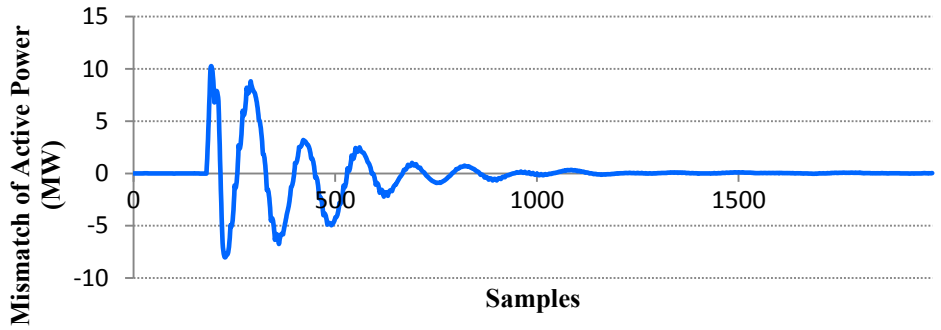

(a)

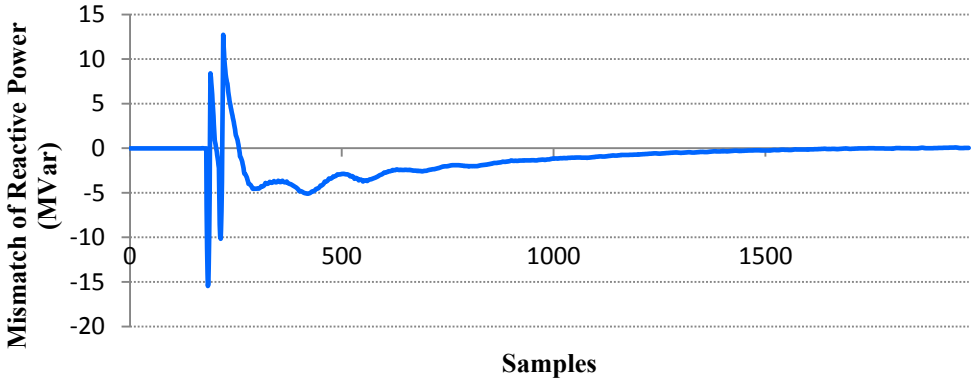

(b)

Figure 3.5 The Mismatch of Simulation Results (a) Real Power (b) Reactive Power

3.3 Load Injection Method

A relatively simple method is proposed [19] to replace the phase shift method by converting measurement data into equivalent impedance. However, this method is not suitable to apply directly with dynamic simulation software, since it only accepts using impendence as a loading. Based on the equivalent impedance method, we proposed an accurate method called “Dynamic Load Injection” to seamlessly integrate with the dynamic simulation software. The

synchronized measurements at the boundary buses are converted to an equivalent Load, as shown in Figure 3.6.

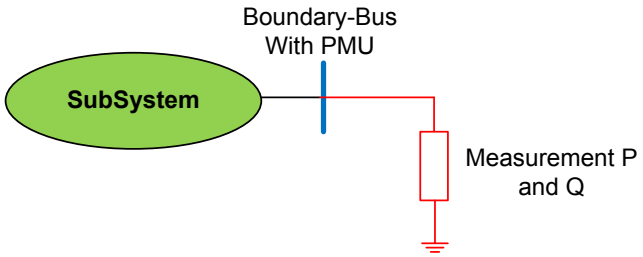

Figure 3.6 Load Injection Method of Hybrid Simulation

The equivalent loading can be calculated at each time step as follows:

$$\begin{cases} P_{sim}(t) = \dfrac{P_{rec}(t)}{V_{rec}^{\ 2}(t)} \times V_{base}^{\ 2} \\ Q_{sim}(t) = \dfrac{Q_{rec}(t)}{V_{rec}^{\ 2}(t)} \times V_{base}^{\ 2} \end{cases} \tag{3.3}$$

where $V_{rec}(t)$, $P_{rec}(t)$ and $Q_{rec}(t)$ are recorded voltage, active and reactive power from PMUs. The V_{base} is the base voltage on the PMU measurement bus. The $P_{sim}(t)$ and $Q_{sim}(t)$ are equivalent loads used in simulation.

From (3.3), one can see that the boundary loads, $P_{sim}(t)$ and $Q_{sim}(t)$, are changed based on the synchronized measurements at each simulation time step. The characteristic of this variable load method is to replace the power system outside the boundary bus by a dynamic load injection based on PMU measurements at each simulation step. It is not difficult to deal with the impedance load in the current commercial power system simulation software. Commercially available simulation software, PSS/E, is applied in this dissertation to implement

this proposed dynamic load injection method. The same test case in the previous section is performed and the mismatch between simulation results (Sim) and record data (Rec) of real power, reactive power, voltage, and angle is shown in Figure 3.7 (a), (b) and Figure 3.8 (a), (b) respectively. Both active and reactive powers are matched very well. From Figure 3.8 (b), it can be noted that the mismatches of the angle are significant, though the curve trends are similar. Because of this mismatch, the sensitivities of both the active and reactive powers corresponding to these parameters are impeded.

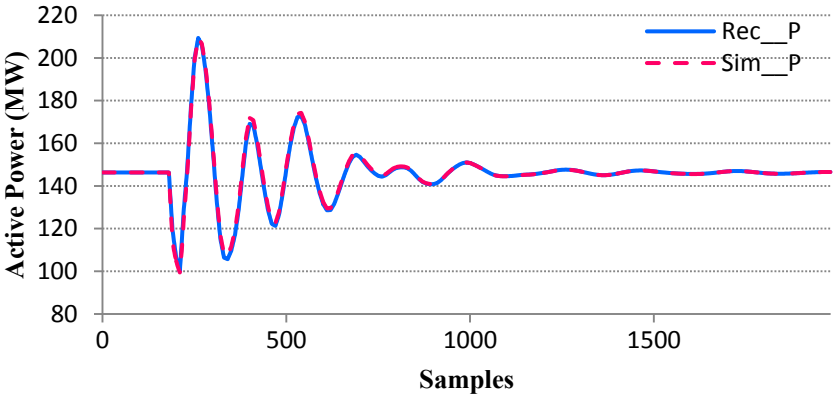

(a)

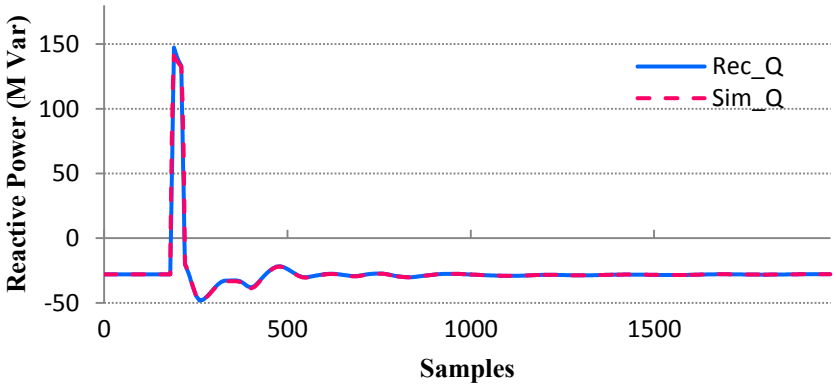

(b)

Figure 3.7 Comparison of Simulation Result and Record Data (a) Real Power (b) Reactive power

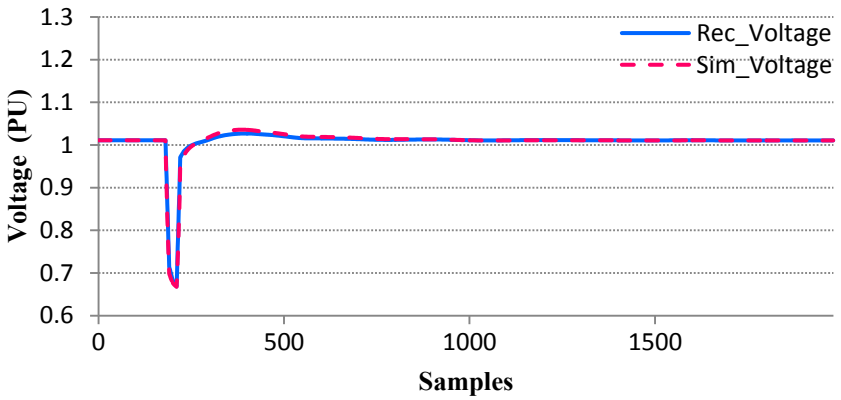

(a)

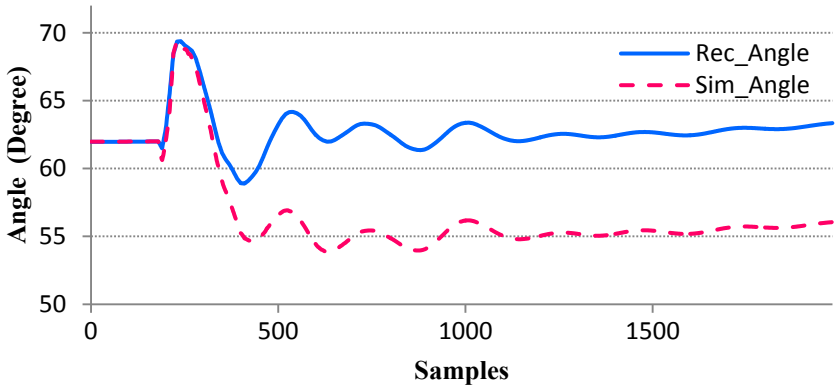

(b)

Figure 3.8 Comparison of Simulation Result and Record Data (a) Voltage (b) Angle

3.4 Conclusion of Hybrid Dynamic Simulation

The hybrid dynamic simulation was first developed for model verification purpose. Since the system outside the PMU measurement boundary buses can be reliably equivalent with PMU measurements, the simulation mismatch caused by outside system can be avoided and only the models inside of boundary buses need to be considered.

The implementation method can be classified into two categories, Load-injection approach and Voltage-injection approach. The Load-injection approach can get a better simulation result than the voltage-injection approach when mismatch of real power and reactive power are used as comparison objective function. However, the former approach will lead to a poor simulation result of voltage and angle measurements. Therefore, voltage-injection approach can represent the system response more due to a parameter change. In other words, voltage-injection is more suitable for the implementation of model parameter identification.

CHAPTER 4

PARAMETERS ANALYSIS AND KEY PARAMETERS IDENTIFICATION

Dozens of parameters in generator unit's models, including generator, exciter, power system stabilizer, and governor make the identification problem more complicated and less efficient. Fortunately, not all of the parameters are critical enough to be incorporated in the estimation problem. The parameters are generally classified into three categories in terms of the purpose of identification.

- The zero parameters. Some parameters are set as zero to represent the absence of the corresponding sub-block in the model.
- The non-significant parameters (except zero parameters) which have trivial impact on the result of dynamic response.
- The key parameters (except zero parameters) which have significant impact on the dynamic response.

The zero parameters and the non-significant parameters are excluded from the parameter identification process since they are not critical, or not used. Only the key parameters are going to be estimated. Thus, the computation burden of the parameter estimation problem can be tremendously reduced. Furthermore, parameter correlation is a common problem for power system parameter identification, which results in non-unique parameter values. The system's extreme correlation existence causes it much difficultly to uniquely estimate the parameters of generator unit. Extreme parameter correlation often hampers calibration of the generator unit's model. Therefore, a parameter correlation analysis is necessary to get an insightful interpretation of the estimated results. The following sections provide detailed

approaches to deal with the problems of key parameters screening and parameter correlation analysis.

4.1 Key Parameter Screening by Trajectory Sensitivity

Some parameters have to be adjusted to reduce the mismatch between the measurements and the simulation response. However, it is not simple to identify which parameters are creating the mismatch. Trajectory sensitivities can provide a way of quantifying the variation of a trajectory corresponding to small changes in the parameters, as in [32] [33] [34].

4.1.1 Trajectory Sensitivity Analysis

Most of power system models can be described by a set of differential and algebraic equations with the form of

$$\begin{cases} \dfrac{dx}{dt} = f(x, y, \lambda) \\ 0 = g^{-}(x, y, \lambda) = g^{+}(x, y, \lambda) \end{cases} \tag{4.1}$$

Where x are the dynamic state variables, y are the algebraic state variables, and λ are parameters. The initial conditions of (4.1) are given by $x(t_0) = x_0$, $y(t_0) = y_0$

For reason of compactness, the following definitions are used

$$\begin{cases} X = \begin{bmatrix} x \\ \lambda \end{bmatrix} \\ F = \begin{bmatrix} f \\ 0 \end{bmatrix} \end{cases} \tag{4.2}$$

With above definition, Equations (4.2) can be rewritten in a compact form as

$$\begin{cases} \dfrac{dX}{dt} = F(X, y) \\ 0 = g^{-}(X, y) = g^{+}(X, y) \end{cases} \tag{4.3}$$

The initial conditions of (4.3) are given by $X(t_0) = X_0$, $y(t_0) = y_0$

The time interval of simulation is selected to be the same as the sampling period of the PMU and it is assumed that the system is smooth ($g^{+}(t_0) = g^{-}(t_0)$). The sensitivities $X_{X_0}(t)$ and $y_{X_0}(t)$ on the time intervals can be derived from partial differentiating of (4.3) with respect to the initial conditions X_0 . The results are shown in (4.4) and (4.5):

$$\frac{\partial \dot{X}}{\partial X_0} = \frac{\partial F(X,y)}{\partial X}\frac{\partial X}{\partial X_0} + \frac{\partial F(X,y)}{\partial y}\frac{\partial y}{\partial X_0} \tag{4.4}$$

$$0 = \frac{\partial g(X,y)}{\partial X}\frac{\partial X}{\partial X_0} + \frac{\partial g(X,y)}{\partial y}\frac{\partial y}{\partial X_0} \tag{4.5}$$

where $\frac{\partial F(X,y)}{\partial X}$, $\frac{\partial F(X,y)}{\partial y}$, $\frac{\partial g(X,y)}{\partial X}$ and $\frac{\partial g(X,y)}{\partial y}$ are time-varying matrices and are calculated along the system trajectories. Initial conditions of $\frac{\partial X}{\partial X_0}(t_0)$ are equal to I which is the identity matrix. Using (4.5) and assuming that it is non-singular along the trajectories, initial condition for $\frac{\partial y}{\partial X_0}$ can be calculated as

$$\frac{\partial y}{\partial X_0} = [\frac{\partial g(X,y)}{\partial y}]^{-1}\frac{\partial g(X,y)}{\partial X} \tag{4.6}$$

Therefore, the trajectory sensitivities $X_{X_0}(t)$ and $y_{X_0}(t)$ can be obtained by solving (4.4) and (4.5) simultaneously with (4.6) using the numerical method with the initial conditions.

Since the simulation time step is very small, the perturbed trajectories can be expressed as (4.7). The estimation is based on first-order approximation and higher order terms are neglected.

$$\begin{cases} \Delta X(t) \approx \dfrac{\partial X(t)}{\partial X_0} \Delta X_0 \\ \Delta y(t) \approx \dfrac{\partial y(t)}{\partial X_0} \Delta X_0 \end{cases} \tag{4.7}$$

For parameter identification problems, the two most important values are active and reactive power at the PMU measurement bus. It is necessary to obtain the sensitivity of the flows P and Q to both initial conditions and parameter variations:

$$\begin{cases} \Delta P(t) = \dfrac{\partial P(t)}{\partial X_0} \Delta X_0 = P_{X_0}(t) \Delta X_0 \\ \Delta Q(t) = \dfrac{\partial Q(t)}{\partial X_0} \Delta X_0 = Q_{X_0}(t) \Delta X_0 \end{cases} \tag{4.8}$$

Note that sensitivities incorporate parameters λ to X_0. Therefore, the sensitivity of the flow to X_0 fully describes its sensitivity to x_0 and λ.

A program has been developed to derive above trajectories for key parameter screening process. Moreover, a study case based on a new installed generator unit in the ERCOT system is created for verification. The generator unit includes generator, governor, exciter, and power system stabilizer to which corresponding models are GENROU, IEESGO, ESAC1A, and PSS2A, respectively. The real power corresponding trajectories are shown in Figure 4.1, Figure 4.2, and the reactive power corresponding trajectories are shown in Figure 4.3, Figure 4.4. Mean square errors as shown in (4.9) are used to be an index for key parameter screening, which is shown in upper-right hand corner of each figure.

$$MSE = \frac{1}{n} \sum_{t=i}^{n} P^2(t) \quad \text{or} \quad MSE = \frac{1}{n} \sum_{t=i}^{n} Q^2(t) \tag{4.9}$$

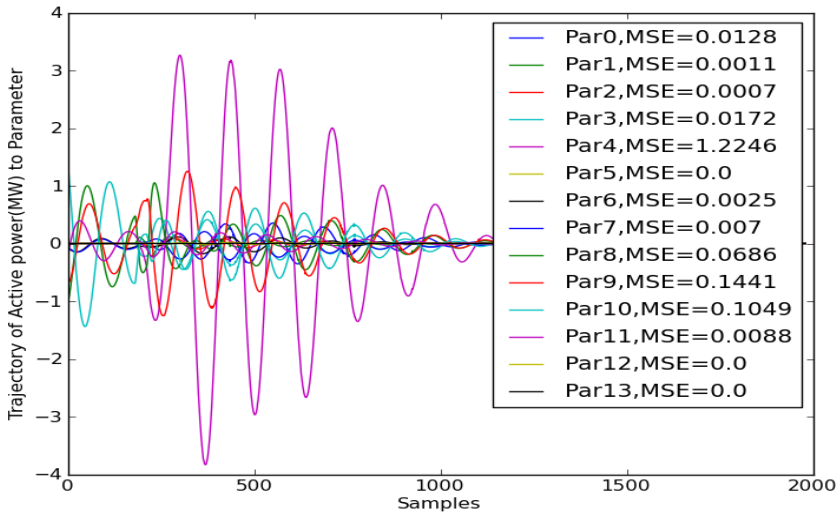

(a)

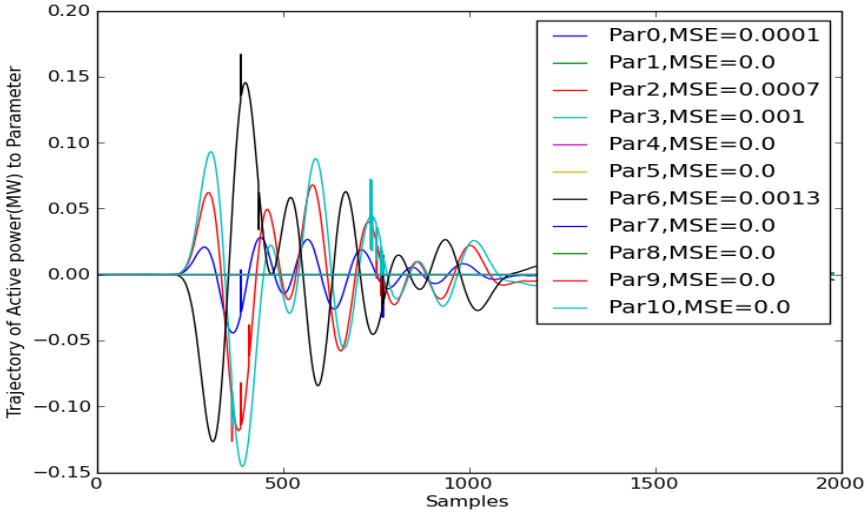

(b)

Figure 4.1 Active Power Trajectory Sensitivity of Models (a) GENROU (b) IEESGO

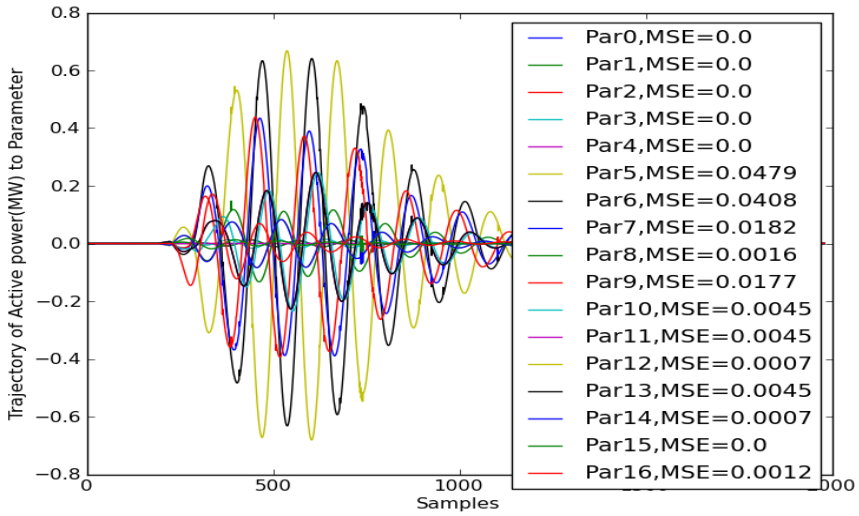

(a)

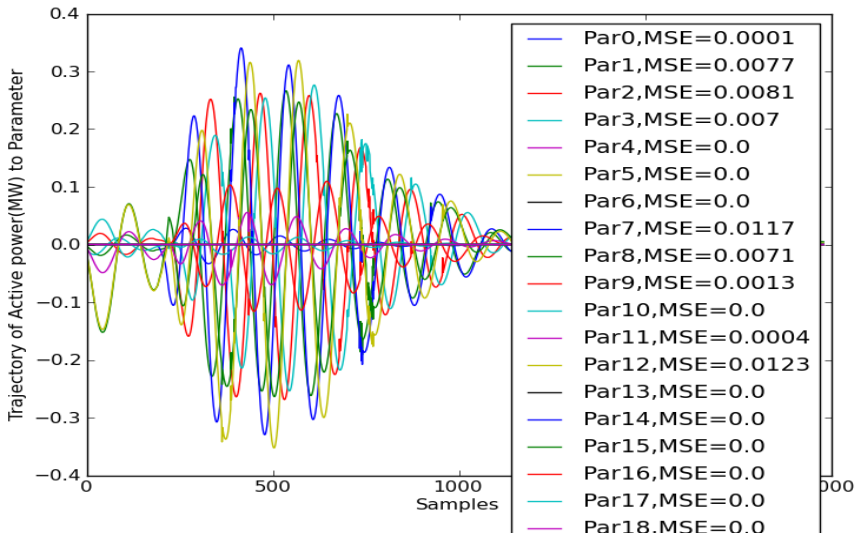

(b)

Figure 4.2 Active Power Trajectory Sensitivity of Models (a) ESAC1A (b) PSS2A

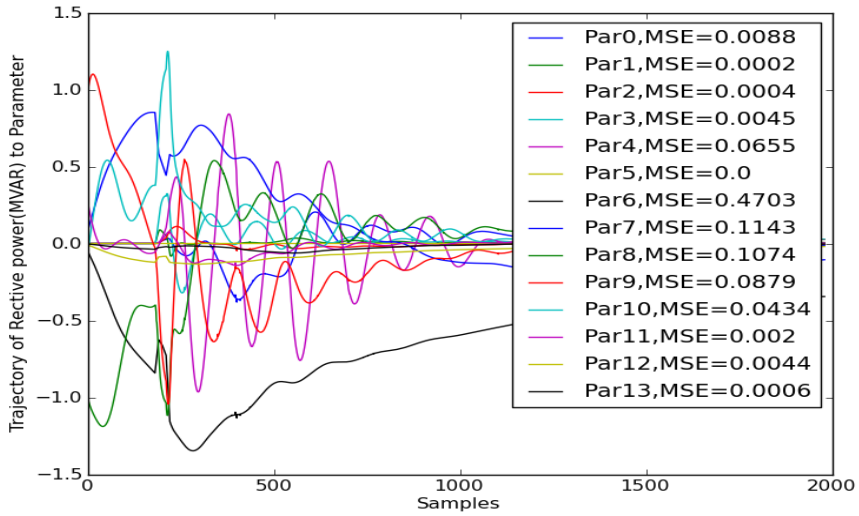

(a)

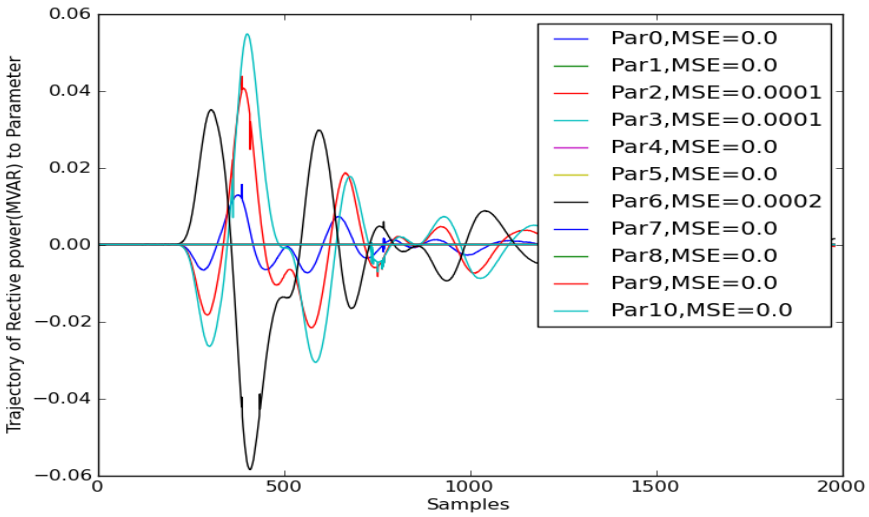

(b)

Figure 4.3 Reactive Power Trajectory Sensitivity of Models (a) GENROU (b) IEESGO

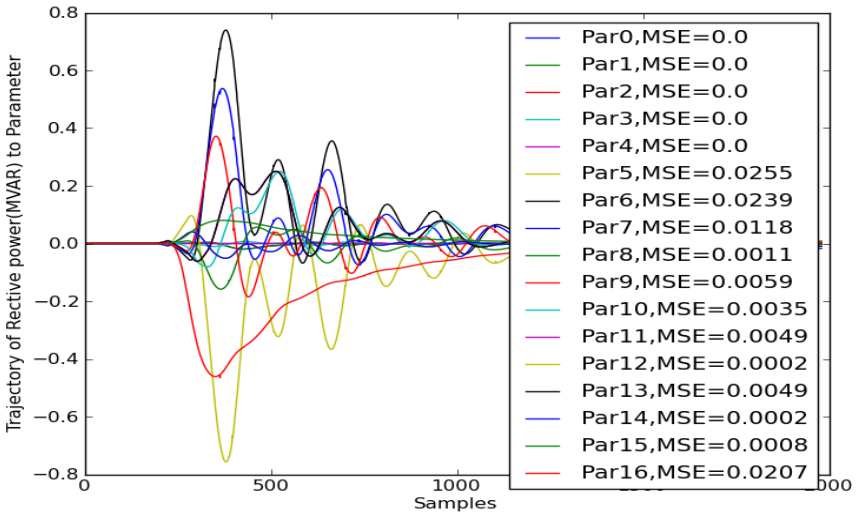

(a)

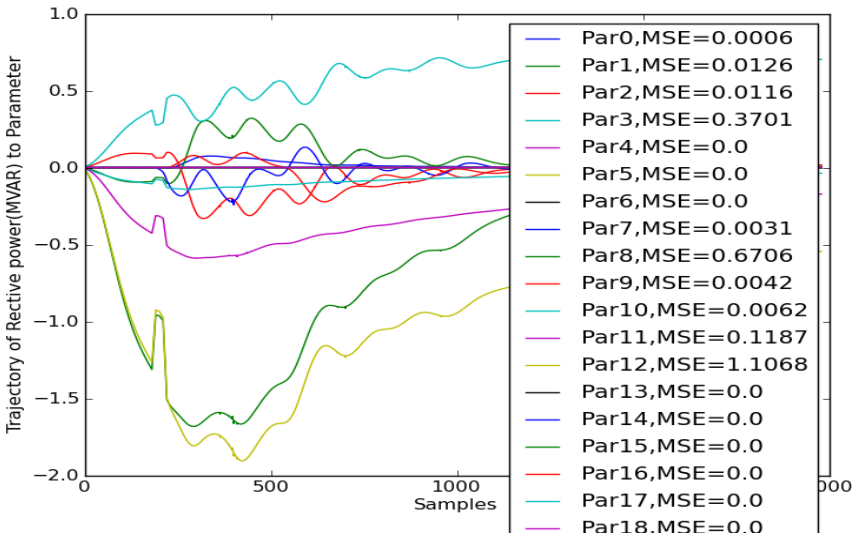

(b)

Figure 4.4 Reactive Power Trajectory Sensitivity of Models (a) ESAC1A (b) PSS2A

4.1.2 Key Parameters

As indicated in the previous subsection, the trajectories $\Delta P(t)$ and $\Delta Q(t)$ which are obtained by using dynamic simulation shown in Figure 4.1 and Figure 4.2 can be used to guide the search for key parameters, i.e., the parameters that are good candidates for the parameter estimation process. If a parameter has a large influence on the trajectory of a particular state, then its corresponding trajectory sensitivity will be large. This kind of parameter can be classified as "Key Parameters." For example, referring to (4.8), if the parameter corresponding to the element i of X_0 has a distinct influence on the trajectory of state P or Q, then the trajectory sensitivity $P_{X_0}(t)$, $Q_{X_0}(t)$ will take on observable values over time.

Large trajectory sensitivities are important because they can give the corresponding parameters a strong influence in adjusting the model trajectory to better match the measured response. On the other hand, the small trajectory sensitivities mean that large change in parameter values is required to get a notable trajectory change. It is important that only parameters which influence measured states can be identified. A parameter may have a significant influence on the system behavior. But if that influence is not observable in the measured states, then the parameter is not identifiable. According to the trajectory results, the key parameters are shown in Table 4.1, where the threshold criterion is 0.05.

Table 4.1 The List of Generator Model's Parameter and Corresponding MSE Value (GENROU)

CONs	Parameter	MSE of Δ P	MSE of Δ Q	Key Parameter
J	T´do	0.0128	0.0088	X
J+1	T´'do	0.0011	0.0002	
J+2	T´qo	0.0007	0.0004	
J+3	T"qo	0.0172	0.0045	X
J+4	H, Inertia	1.2246	0.0655	X
J+5	D, damping	0.0	0.0	

Table 4.1 – *Continued*

J+6	Xd	0.0025	0.4703	X
J+7	Xq	0.007	0.1143	X
J+8	X´d	0.0686	0.1074	X
J+9	X´q	0.1441	0.0879	X
J+10	X”d = X”q	0.1049	0.0434	X
J+11	Xl	0.0088	0.002	X
J+12	S(1.0)	0.0	0.0044	X
J+13	S(1.2)	0.0	0.0006	X

Table 4.2 The List of Governor Model’s Parameter and Corresponding MSE Value (IEESGO)

CONs	Parameter	MSE of Δ P	MSE of Δ Q	Key Parameter
J	T1	0.0001	0.0	
J+1	T2	0.0	0.0	
J+2	T3	0.0007	0.0001	
J+3	T4	0.001	0.0001	
J+4	T5	0.0	0.0	
J+5	T6	0.0	0.0	
J+6	K1	0.0013	0.0002	
J+7	K2	0.0	0.0	
J+8	K3	0.0	0.0	
J+9	P_{MAX}	0.0	0.0	
J+10	P_{MIN}	0.0	0.0	

Table 4.3 The List of Exciter Model’s Parameter and Corresponding MSE Value (ESAC1A)

CONs	Parameter	MSE of Δ P	MSE of Δ Q	Key Parameter
J	TR	0.0001	0.0006	
J+1	TB	0.0077	0.0126	X
J+2	TC	0.0081	0.0116	X
J+3	KA	0.007	0.3701	X
J+4	TA	0.0	0.0	
J+5	VA_{MAX}	0.0	0.0	
J+6	VA_{MIN}	0.0	0.0	

Table 4.3 – *Continued*

J+7	TE > 0	0.0117	0.0031	X
J+8	KF	0.0071	0.6706	X
J+9	TF > 0	0.0013	0.0042	X
J+10	KC	0.0	0.0062	X
J+11	KD	0.0004	0.1187	X
J+12	KE	0.0123	1.1068	X
J+13	E1	0.0	0.0	
J+14	SE(E1)	0.0	0.0	
J+15	E2	0.0	0.0	
J+16	SE(E2)	0.0	0.0	
J+17	VR_{MAX}	0.0	0.0	
J+18	VR_{MIN}	0.0	0.0	

Table 4.4 The List of Power System Stabilizer Model's Parameter and Corresponding MSE Value (PSS2A)

CONs	Parameter	MSE of ΔP	MSE of ΔQ	Key Parameter
J	Tw1 (>0)			
J+1	Tw2			
J+2	T6	0.0	0.0	
J+3	Tw3 (>0)			
J+4	Tw4	0.0	0.0	
J+5	T7	0.0479	0.0255	X
J+6	KS2	0.0408	0.0239	X
J+7	KS3	0.0182	0.0118	X
J+8	T8	0.0016	0.0011	
J+9	T9 (>0)	0.0177	0.0059	X
J+10	KS1	0.0045	0.0035	X
J+11	T1	0.0045	0.0049	X
J+12	T2	0.0007	0.0002	
J+13	T3	0.0045	0.0049	X
J+14	T4	0.0007	0.0002	
J+15	VST_{MAX}	0.0	0.0008	
J+16	VST_{MIN}	0.0012	0.0207	

4.2 Parameters Correlation Analysis by Singular Value Decomposition (SVD)

Parameter correlation is a common issue for power system parameter identification problems and results in non-unique estimated parameter values. i.e., it is impossible to uniquely estimate the parameters of generator unit, when the system extreme correlation exists. Extreme parameter correlation often restrains calibration of the generator unit's mode, regardless of how models are calibrated. However, the accuracy of results can be dramatically improved by using associated statistics and parameter correlation analyses.

One convenient method to indicate the parameter correlation is the correlation coefficient. However, reference [35] notes some problems about using parameter correlation coefficients to detect parameter correlation. Such as, if the element of sensitivity metric has too many errors or the calculated correlation coefficients are corrupted and can no longer have sufficient precision to identify. Furthermore, the correlation coefficient can only identify correlation between pairs of parameters and is not able to determine the extent of correlation when more than two parameters are correlated. The following presents a brief review of some important facts about the Singular Value Decomposition (SVD) and how the SVD might assist the parameter correlation analysis.

4.2.1 Properties of the SVD

The fundamental treatment of SVD is referred to $[36]$ and interpreted as follows:

Any rectangular matrix, X, with m rows and n columns can be written as :

$$X = USV^T \tag{4.10}$$

where U is an orthogonal m by m matrix, i.e. $U^TU = UU^T = \mathrm{I}_{m\times m}$,

V is an orthogonal n by n matrix, i.e. $V^TV = VV^T = I_{n\times n}$, and

S is an m by n matrix containing non-negative numbers (the singular values) on the diagonal and zeros outside the diagonal.

The column vectors $\{u_i\}$ of U are called left-singular vectors, the column vectors $\{v_i\}$ of V are called right-singular vectors, and the diagonal elements $\{\sigma_i\}$ of S are the singular values. Here is the discussion about how to interpret the results from the SVD.

The singular values: The number of singular values equals to the number of parameters. If one or more singular values are zero or very small, this indicates that two or more of the columns of X are linearly dependent and two or more of the parameters are extremely correlated.

The right-singular vectors: There is one right-singular vector corresponding to one singular value, and in each right-singular vector there is one component for each parameter. If extreme correlation is indicated by one or more than one of very small singular values, then the right-singular vectors corresponding to the small singular values are particularly meaningful.

The null space: The components in the corresponding right-singular vector with small absolute values correspond to parameters which are not correlated and therefore can be uniquely estimated. Components with large absolute values correspond to parameters which are correlated and therefore cannot be uniquely estimated.

4.2.2 Apply SVD in Parameters Correlation Analysis

Consider the same example using trajectory sensitivity analysis. Since only key parameters are taken into account for further calibration, the sensitivity matrix, X, is built by the active power trajectories which are corresponding to key parameters. The key parameters are listed in the first column of Table 4.5. The sensitivity matrix, X, SVD decomposed results are shown as Table 4.5.

Table 4.5 SVD Decomposition Results

Parameter	v_1	v_2	v_3	v_4	v_5	v_6	v_7	v_8	v_9	v_{10}	v_{11}	v_{12}	v_{13}	v_{14}	v_{15}	v_{16}	v_{17}	v_{18}	v_{19}	v_{20}	v_{21}
H, Inertia	-0.057	0.165	-0.119	0.116	-0.101	0.119	-0.031	0.299	-0.090	0.375	-0.279	0.370	-0.167	0.062	0.456	-0.030	0.059	-0.019	-0.173	-0.400	-0.172
KE	0.101	0.027	-0.018	-0.252	-0.003	-0.138	-0.009	-0.151	0.155	0.049	-0.558	-0.429	-0.193	0.192	0.145	-0.261	-0.417	0.120	0.030	0.030	-0.085
KF	-0.938	0.216	0.147	-0.120	0.036	-0.088	-0.043	-0.121	0.094	0.034	0.014	-0.032	-0.016	0.003	-0.011	-0.028	0.005	0.013	-0.008	-0.005	-0.002
Xd	-0.033	0.023	0.022	-0.010	-0.109	-0.356	0.331	-0.059	-0.237	-0.619	-0.206	0.051	0.043	-0.049	0.232	0.372	-0.032	-0.060	-0.032	-0.242	-0.033
KA	0.063	-0.029	0.025	-0.011	-0.151	-0.322	0.598	0.039	0.615	0.159	0.093	0.119	-0.133	-0.004	-0.037	-0.124	0.218	0.012	-0.015	-0.006	0.039
X´q	-0.066	-0.215	-0.539	-0.524	-0.418	-0.125	-0.181	-0.019	-0.067	0.070	0.112	0.104	-0.214	0.071	-0.159	0.212	0.043	0.048	-0.042	0.014	0.015
X´d	-0.213	-0.549	-0.114	0.684	-0.203	-0.175	-0.126	0.049	0.030	0.019	-0.078	-0.134	-0.168	0.086	-0.056	0.043	-0.105	0.060	-0.008	0.030	-0.013
X”d = X”q	0.162	0.257	0.633	0.027	-0.445	-0.108	-0.261	0.011	0.005	0.053	0.045	0.032	-0.327	0.119	-0.170	0.249	-0.020	0.083	-0.049	0.012	0.004
Xq	-0.012	0.085	-0.120	0.039	0.556	0.158	0.160	0.115	0.049	-0.011	0.010	-0.063	-0.534	0.204	-0.236	0.434	-0.041	0.112	-0.100	-0.040	0.005
KD	0.034	0.399	-0.303	0.238	-0.166	0.115	-0.052	-0.156	0.110	-0.117	-0.072	-0.096	-0.249	-0.699	-0.070	-0.032	-0.019	0.112	-0.061	0.075	-0.066
T7	-0.026	-0.369	0.286	-0.223	0.179	-0.166	0.093	0.151	-0.253	0.116	-0.038	0.153	-0.115	-0.490	-0.240	-0.207	-0.203	0.220	-0.227	-0.202	0.049
KS2	-0.048	-0.229	0.166	-0.157	0.032	0.070	0.004	0.229	0.069	0.213	-0.363	-0.149	0.065	-0.327	0.162	0.431	0.275	-0.153	0.199	0.392	-0.127
T9	-0.002	-0.061	0.007	0.046	-0.074	0.264	0.026	-0.342	0.155	0.022	-0.499	0.212	0.306	0.089	-0.418	0.140	0.118	-0.022	-0.389	-0.101	0.105
VST_{MIN}	0.006	0.180	-0.094	0.037	-0.005	-0.212	-0.059	0.321	-0.057	0.078	-0.145	-0.237	0.044	-0.039	-0.462	-0.079	0.051	-0.554	0.230	-0.363	0.037
T”qo	-0.019	-0.180	0.087	-0.025	-0.022	0.280	0.048	-0.329	0.092	-0.027	-0.062	0.349	-0.191	-0.071	-0.041	0.015	-0.173	-0.070	0.707	-0.239	-0.031
T´do	0.021	-0.158	0.092	-0.050	0.108	-0.004	-0.108	-0.280	-0.149	-0.194	-0.082	0.023	-0.463	0.033	0.104	-0.356	0.507	-0.384	-0.165	0.101	-0.003
TB	-0.029	0.208	-0.106	0.090	0.041	-0.212	0.018	0.250	-0.213	-0.110	-0.331	0.424	-0.038	0.138	-0.194	-0.210	0.070	0.235	0.254	0.454	0.218
TC	-0.062	0.006	0.024	0.009	-0.250	0.305	0.366	0.011	-0.370	0.094	-0.038	-0.405	-0.029	0.084	-0.071	-0.095	0.379	0.384	0.172	-0.181	0.137
TE	-0.015	0.017	0.006	0.015	-0.043	0.009	0.162	-0.011	-0.140	-0.032	0.040	0.062	0.052	0.103	-0.265	-0.100	0.012	0.036	-0.006	0.130	-0.913
XI	-0.086	0.018	0.020	0.021	-0.252	0.298	0.435	0.047	-0.242	0.097	0.069	0.037	-0.121	0.023	0.003	-0.021	-0.436	-0.453	-0.173	0.331	0.154
Singular Value	***51.773***	***19.313***	***16.188***	***9.535***	***5.827***	***2.290***	***1.567***	***1.291***	***1.081***	***0.594***	***0.479***	***0.419***	***0.345***	***0.271***	***0.186***	***0.120***	***0.108***	***0.091***	***0.078***	***0.067***	***0.045***

The right-singular vectors are shown in Table 4.5, where the last row notes the singular values. In normal cases, when the singular values drop below 5% of the maximum, it is difficult to calibrate parameters uniquely. Hence, the models here with the maximum of 5 parameters among 21 parameters might be accurately calibrated, the others are highly correlated. Moreover, the small singular values which near zero provide the correlation among two or more parameters. For example, form the correlation equation from the last 6 columns as follows:

$$\Delta v_{21} = 0.218\Delta TB - 0.913\Delta TE + \cdots \quad).045 \tag{4.11}$$

$$\Delta v_{20} = -0.400\Delta H - 0.242\Delta Xd - 0.202\Delta T7 + 0.392\Delta KS2 - 0.363\Delta VST - 0.239\Delta T''q0 + 0.454\Delta TB + 0.331\Delta XI + \cdots \quad).067 \tag{4.12}$$

$$\Delta v_{19} = -0.227\Delta T7 - 0.389\Delta T9 + 0.707\Delta T''q0 + 0.254\Delta TB + \cdots \quad).078 \tag{4.13}$$

$$\Delta v_{18} = 0.220\Delta T7 - 0.554\Delta VST - 0.384\Delta T'd0 + 0.235\Delta TB + 0.384\Delta TC - 0.453\Delta X1 + \cdots \quad).091 \tag{4.14}$$

$$\Delta v_{17} = -0.417\Delta KE - 0.218\Delta KA - 0.203\Delta T7 + 0.275\Delta KS2 - 0.507\Delta T'd0 - 0.379\Delta TC - 0.436\Delta XI + \cdots \quad).108 \tag{4.15}$$

$$\Delta v_{16} = -0.261\Delta KE + 0.372\Delta Xd + 0.212\Delta X'q + 0.249\Delta X''q + 0.434\Delta Xq - 0.207\Delta T7 + 0.431\Delta KS2 - 0.356\Delta T'd0 - 0.210\Delta TB + \cdots \quad).120 \tag{4.16}$$

Equation (4.11) interpreted that parameters *TB* and *TE* are correlated. In other words, the simulation output response could reached the same level by tuning either *TB* or *TE*. Similarly, from (4.12), we can note that parameters *H, Xd, T7, KS2, VST,* $T''q0$, *TB,* and *XI* are correlated. The conclusion results are shown in Table 4.5. The values shown in red are the magnitude of the components with large absolute values in the corresponding right-singular vector. The values give information on the extent of the correlation and shown which parameters cannot be uniquely estimated.

4.3 Conclusion of Parameters Analysis

This study used trajectory sensitivity analysis extracting out 21 key parameters which are listed in Table 4.6. The parameters with the higher MSE of sensitivity can be easily calibrated. However, this example has 16 very small singular values, and some parameters are correlated. Therefore, they cannot be uniquely estimated. Those parameters are the magnitude of the components with large absolute values in the corresponding right-singular vector. The parameters with higher sensitivity can be estimated more precisely. In contrast, the parameter correlation hampers the accuracy of the estimated results. Therefore, according to corresponding sensitivity and correlation of each parameter, the identifiability of parameters can be classified into three categories, high, medium, and low, as shown in Table 4.6. The identifiability can be an index of the accuracy of expected results.

Table 4.6 The List of Correlation and Identifiability of Key Parameter

Parameters	MSE of Trajectory	Correlation	identifiabilty
H	1.2901	X	High
KE	1.1191	X	High
KF	0.6777		High
Xd	0.4728	X	High
KA	0.3771		High
X´q	0.2320		High
X´d	0.1760		High
X”d = X”q	0.1483		High
Xq	0.1213	X	Medium
KD	0.1191	X	Medium
T7	0.0734	X	Low
KS2	0.0647	X	Low
KS3	0.0300		Medium
T9	0.0236	X	Low

Table 4.6 – *Continued*

VST_{MIN}	0.0219	X	Low
T”qo	0.0217	X	Low
T´do	0.0216	X	Low
TB	0.0203	X	Low
TC	0.0197	X	Low
TE	0.0148		Medium
Xl	0.0108	X	Low

After identifying the level of parameter’s identifiability and whether a correlation exists, a multi-dimension optimization algorithm is proposed to find a set of best fitting parameters.

CHAPTER 5

OPTIMIZATION ALGORITHM

The objective of this dissertation is to make the simulation results match with the measured curve by identifying accurate parameters of devices in a power system. As described in Chapter 2, the conventional optimization methods depend upon on the quality of the initial guess. The intelligent method is not affected by the initial guess, but it requires many time-consuming fitness evaluations, because of the need to perform the dynamic simulation. Therefore, a new intelligent optimization method known as the SPSA-PSO cooperative method proposes the using of second–order SPSA along with an inexact line search in order to accelerate the convergence of the PSO while maintaining the advantageous global search ability it possesses. This method is proposed and described below.

5.1 Particle Swarm Optimization

A stochastic population-based intelligent optimization algorithm, Particle Swarm Optimization (PSO) was originally developed in 1995 by Kennedy and Eberhart as a novel intelligent optimization method. The optimized solution is achieved through the mathematical simulation of the social behavior of a flock of birds. Since 1999, power system researchers have applied the PSO technique to solve optimization problems in many areas such as economic dispatch, reactive power and voltage control, state estimation, as well as load flow and optimal power flow [5]. PSO is based on the swarm concept, that is, each particle represents a candidate solution and has two properties: position (x_i) and velocity (v_i) which direct the flight of the particle. A population of particles, called a swarm, keeps flying around the search space until the stop criteria is satisfied.

A variety of PSO algorithms have evolved since the technique's first development [37]. In the basic global best PSO algorithm, each particle in the swarm is randomly initialized in the problem space. At each step, each particle is updated according to the formulas:

$$v_i^{k+1} = wv_i^k + c_1 r_1 (p_{best\,i}{}^k - x_i^k) + c_2 r_2 (g_{best}{}^k - x_i^k) \tag{5.1}$$

$$x_i^{k+1} = \begin{cases} x_i^k + v_i^{k+1} & if\ f(x_i^{k+1}) < f(x_i^k) \\ x_i^k & if\ f(x_i^{k+1}) \geq f(x_i^k) \end{cases} \tag{5.2}$$

where v_i^k is the velocity vector of particle *i* in dimension *i=1,...,p* at iteration *k*

x_i^k is the position of particle *i* in dimension *i=1,...,p* at iteration *k*

c_1 and c_2 are two positive acceleration constants used to scale the contribution of the *cognitive* and *social* components respectively

w is the inertia weight and can be define as a linear decreasing sequence as below $w(k) = w_{\max} - k(w_{\max} - w_{\min}) / (k_{\max} + 1)$, where $w_{\max}$ is the largest inertia weight (usually 0.9), $w_{\min}$ is the smallest inertia weight (usually 0.4), and $k_{\max}$ is the maximum iterations number.

r_1 and r_2 are two random numbers in range [0, 1]

$p_{best\,i}{}^k$ is the personal best position associated with particle *i.* this is the best position the particle has visited since the first iteration

$g_{best}{}^k$ is the best position of the whole swarm after *k* iterations.

One of the main advantages of PSO is that this method can explore multiple solutions in parallel and utilizes a cooperative manner to search for the global minimum solution. In addition to this, a good initial guess solution is not required and the algorithm can be easily implemented. However, the drawback of PSO is the slow convergence rate, due to the low driving force of the g_{best} particle, except with inertia weight, w. As shown in (5.1), the first term

in the summation is the only way for g_{best} to update itself. For the generator parameter identification problem, the fitness evaluations are the most burdened by computation. Therefore, a gradient based algorithm, Simultaneous Perturbation Stochastic Approximation (SPSA), could be adopted to improve the effectiveness of this computation.

5.2 Simultaneous Perturbation Stochastic Approximation

The recently developed Simultaneous perturbation stochastic approximation (SPSA) method is used virtually in all areas of engineering, as well as in physical and social sciences [38] [39]. These applied problems are without a closed-form for the solution and the input signals for an optimization problem may be contaminated with noise. Typical applications include: model fitting and statistical parameter estimation, adoptive control, pattern classification, simulation-based optimization, etc. The SPSA's principal benefit is the reduction in the number of objective function evaluations required to achieve a given level of accuracy in the optimization process. Regardless of the dimension of the optimization problem, SPSA needs only two (for the gradient) or four (for the Hessian matrix) objective function estimates in each iteration. Because each objective function evaluation stands for a dynamic simulation which needs to be performed, the aforementioned benefit becomes very important. The dynamic simulation portion of this algorithm requires the highest computational burden, while the other parts of the algorithm are relatively insignificant in terms of computation.

The SPSA algorithm is the general iterating process for an estimate ($\hat{\lambda}_k$) of a solution (λ^*) with dimension *p*. The principal iterations for the first and second-order SPSA algorithms are as follows [39] [40] [41] [42] [43]:

1SPSA:

$$\lambda_{k+1} = \hat{\lambda}_k - a_k \hat{g}_k(\hat{\lambda}_k), \quad k = 0, 1, 2, \cdots \tag{5.3}$$

2SPSA:

$$\hat{\lambda}_{k+1} = \hat{\lambda}_k - \bar{a}_k \bar{\bar{H}}_k^{-1} \hat{g}_k(\hat{\lambda}_k), \quad \bar{\bar{H}}_k = f_k(\bar{H}_k) \tag{5.4}$$

$$\bar{H}_k = \frac{k}{k+1}\bar{H}_{k-1} + \frac{1}{k+1}\hat{H}_k, \quad k = 0, 1, 2, \cdots \tag{5.5}$$

where

a_k and $\bar{a}_k$ are the nonnegative decaying gain sequences that satisfy certain SA conditions,

$\hat{g}_k(\hat{\lambda}_k)$ is the SP estimate of the objective function gradient

$\bar{H}_k$ is the SP estimate of the Hessian matrix

f_k is a mapping function which transfers the usual non-positive-definite $\bar{H}_k$ to a positive-definite $p \times p$ matrix.

Both a_k and $\bar{a}_k$ can be represented by the same as shown in (5.6). However, the constant values *A* and a are different from each other.

$$a_k = \frac{a}{(A + K + 1)^{\alpha}} \tag{5.6}$$

The $\hat{g}_k(\hat{\lambda}_k)$ is shown in (5.7). $\hat{g}_k(\hat{\lambda}_k)$ depends on the gain sequence c_k as shown in (5.11) and a *p*-dimensional random variable, Δ_k, usually chosen as Bernoulli ± 1 distribution.

$$\hat{g}_k(\hat{\lambda}_k) = \frac{f(\hat{\lambda}_k + c_k\Delta_k) - f(\hat{\lambda}_k - c_k\Delta_k)}{2c_k} \begin{bmatrix} \Delta_{k1}^{-1} \\ \Delta_{k2}^{-1} \\ \vdots \\ \Delta_{kp}^{-1} \end{bmatrix} \tag{5.7}$$

The formula for estimating the Hessian matrix ($\bar{H}_k$) at each iteration is

$$\hat{H}_k = \frac{1}{2}\left[\frac{\delta G_k^T}{2c_k\Delta_k} + \left(\frac{\delta G_k^T}{2c_k\Delta_k} \right)^T \right] \tag{5.8}$$

And, let

$$\delta G_k = G_k^{(1)}(\hat{\lambda}_k + c_k\Delta_k) - G_k^{(1)}(\hat{\lambda}_k - c_k\Delta_k) \tag{5.9}$$

where $G_k^{(1)}(\cdot)$ as shown in (5.10) is using one-sided gradient approximation in order to reduce the total number of objective function evaluation.

$$G_k^{(1)}(\hat{\lambda}_k \pm c_k\Delta_k) = \frac{f(\hat{\lambda}_k \pm c_k\Delta_k + \tilde{}}{\tilde{}} \qquad \frac{}{\pm c_k\Delta_k)} \begin{bmatrix} \tilde{} \\ \tilde{} \\ \vdots \\ \tilde{} \end{bmatrix} \tag{5.10}$$

where c_k and $\tilde{}$ are similar as shown in (5.11), a sequence of positive scalars gain sequence generated in the same statistical manner. For instance, the value of *c* could be the standard deviation of the objection evaluation in the first few iterations, and γ is a positive constant value.

$$c_k = \frac{c}{(k+1)^{\gamma}} \tag{5.11}$$

Since the dimension of *p* in this application is not too large, one useful form for f_k is $\bar{\bar{H}}_k = (\bar{H}_k{}^T \bar{H}_k + \delta_k I_p)^{1/2}$; where δ_k is a positive near zero value and I_p is a $p \times p$ identity matrix and other forms for f_k may be useful [13][15] .

From (5.3) and (5.4), we can note that 1SPSA predetermines the gain sequence (a_k) as a step size for every parameters in the whole iteration process, whereas 2SPSA derives a generalized gain sequence ($\bar{a}_k \bar{\bar{H}}_k^{-1}$) adapted to near optimal step size for the different parameters at each given iteration. This is the reason why 2SPSA may outperform 1SPSA. Furthermore, [44] shows that 2SPSA can achieve a nearly optimal solution with a trivial gain sequence ($\bar{a}_k = 1/(k+1)$), which effectively eliminates the troublesome issue of selecting a "good" gain sequence, *A* and a .

Another helpful aspect to note is that SPSA needs only 2-4 measurements, regardless of the dimension of the objective function. This result makes SPSA as the best choice for parameter identification process. Taking into account the advantages of global search ability of PSO, as well as the fast convergence rate, and the less objective function estimations of 2SPSA, a high efficiency global optimization algorithm is presented in this dissertation.

5.3 The Proposed SPSA-PSO Cooperative Method

As mentioned in the previous section, the poor g_{best} particle updating is the major drawback of the PSO algorithm. SPSA can be successfully utilized to steer the g_{best} particle in the right direction, using the objective function gradient estimation, meanwhile, avoiding becoming trapped locally due to its stochastic nature. However, the convergence speed of SPSA becomes decreased over the iteration time. In order to force the optimization algorithm converge to a certain level in finite iterations, an inexact line search method as shown in (5.12) is applied to derive the next iteration solution $\hat{\lambda}_{k+1}$. This is accomplished by searching for the minimum value among the estimated objective values of 2SPSA, which can consequently and effectively enforce the descent of the objective function.

$$\min \begin{cases} f(\hat{\lambda}_k + c_k\Delta_k),\ f(\hat{\lambda}_k - c_k\Delta_k),\ f(\hat{\lambda}_k + c_k\Delta_k + \tilde{} \\ f(\hat{\lambda}_k - c_k\Delta_k + \tilde{} \qquad\qquad _1) \end{cases} \qquad \int \tag{5.12}$$

Using 2SPSA algorithm, four objective function estimations, $f(\hat{\lambda}_k + c_k\Delta_k)$, $f(\hat{\lambda}_k - c_k\Delta_k)$, $f(\hat{\lambda}_k + c_k\Delta_k + \tilde{}$, and $f(\hat{\lambda}_k - c_k\Delta_k + \tilde{}$, are required per iteration, two for the standard gradient estimate $\hat{g}_k(\cdot)$ and two for the one-side gradient $G_k^{(1)}(\cdot)$. Additionally, a blocking process used to prevent the step size from exceeding a certain level is based on one additional objective function estimation, $f(\hat{\lambda}_{k+1})$. i.e., if $f(\hat{\lambda}_{k+1}) - f(\hat{\lambda}_k) > tolerance$, then $\hat{\lambda}_{k+1} = \hat{\lambda}_k$. Therefore,

the inexact line search method can improve the convergence rate through existing five estimated objective functions, without an additional computational cost.

In this integration approach, the internal PSO structure will not be changed. Only the movement of g_{best} particle will be affected. The flow chart of this approach is shown in Figure 5.1. At each iteration of PSO, the g_{best} particle is updated using 2SPSA. Meanwhile, the 2SPSA process takes the PSO's result, g_{best}, as an initial value, and keeps driving the objective function descent. Both processes of PSO and 2SPSA require same number of objective function estimations. For example, a specific PSO has 30 particles; while equally, 2SPSA, which costs five objective function evaluations with each iteration, will take 6 iterations in 30 objective function estimations, as well.

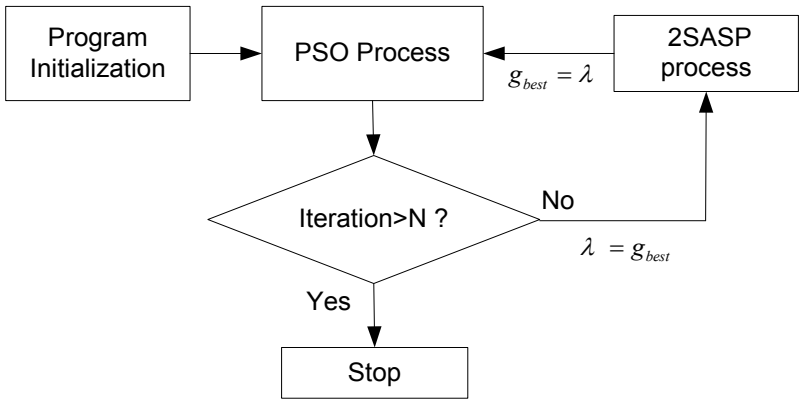

Figure 5.1 The Flow Chart of Cooperation SPSA-PSO

For the application of generator parameter identification, the accuracy of the estimated results and the amount of computational time are critical. This proposed SPSA-PSO cooperative algorithm can provide a balance between convergence and global search ability.

CHAPTER 6

CASE STUDY

This dissertation proposes a new approach and implementation process for solving Phasor Measurement Unit (PMU) based generator unit's parameter identification problems. The implementation scheme established a close link among hybrid dynamic simulation, trajectory sensitivity, and SPSA-PSO cooperative algorithm for parameter identification. The hybrid dynamic simulation is implemented in commercially available software, PSS/E, to create the equivalent of an external-system outside the buses of PMU boundary. This crucial process effectively reduces the burdens of computation and increases the accuracy of the results. Furthermore, trajectory sensitivity is used to provide valuable information for determining key parameters which will be tuned. After this, an enhanced optimization algorithm, Simultaneous Perturbation Stochastic Approximation (SPSA) is used to drive Particle Swarm Optimization (PSO), is proposed for solving parameter identification. This novel algorithm effectively speeds up the convergence rate and maintains the ability to find global minima using the PSO method, thereby dramatically improving the search efficiency and solution quality. The effectiveness and feasibility of the proposed method and processes are demonstrated by a newly installed generator unit in the ERCOT system. In this case study, practical implementation issues are further illustrated. Additionally, the experiment shows encouraging results and verifies that the proposed approach was capable of efficiently determining higher accuracy parameters regarding PMU-based dynamic model parameter identification problems.

In this chapter, we use the assumed test case and data to evaluate the feasibility and effectiveness of the proposed method.

6.1 Case Configuration and Data Set

A newly installed power plant with two identical generators in the ERCOT system is studied as a test case. The power plant is connected to the ERCOT system through a 138kV line, as shown in Figure 6.1. A PMU has been installed in bus # 8126 to record the necessary disturbance signals which it requires to identify the parameter identification problems.

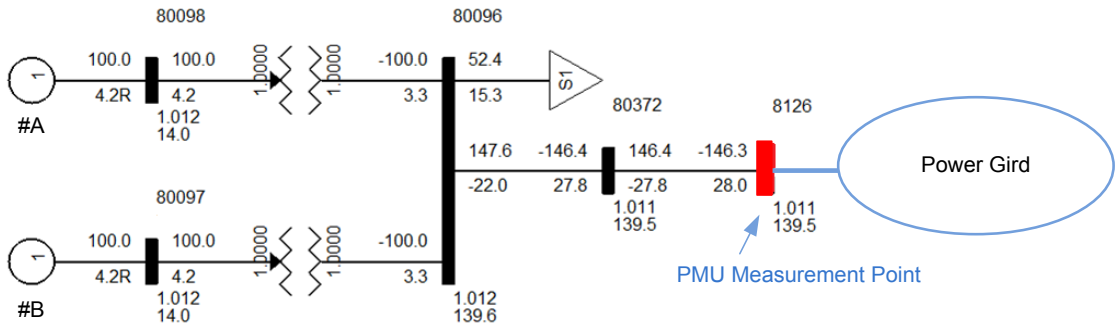

Figure 6.1 One Line Diagram of Local System of the Test Case

The assumed generator unit #A is the parameter estimation target, and the unit's models are used for the generator, governor, exciter, and power system stabilizer (PSS) are "GENROU", "IEESGO", "ESAC1A", and "PSS2A" respectively. The detailed parameters and the block diagram of the models are shown in Figure 6.2. to Figure 6.5.

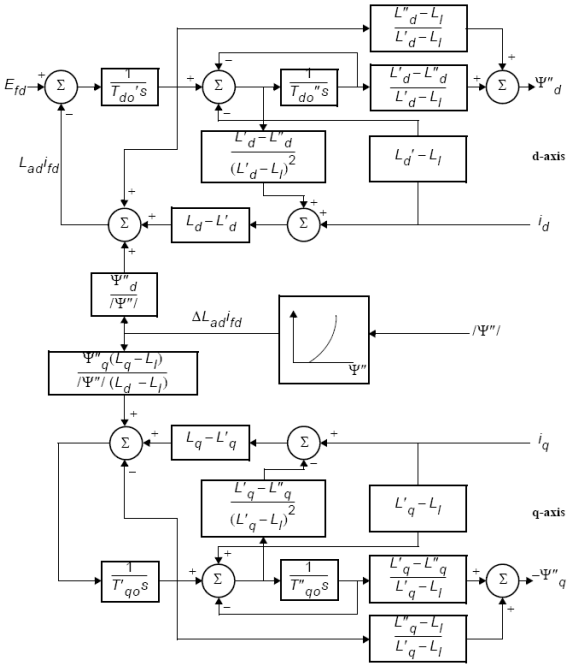

CONs	Description	Value
J	T´do (>0) (sec)	8.4
J+1	T´do (>0) (sec)	0.04
J+2	T´qo (>0) (sec)	2.5
J+3	T"qo (>0) (sec)	0.15
J+4	H, Inertia	4.47
J+5	D, Speed damping	0.0
J+6	Xd	1.98
J+7	Xq	1.88
J+8	X´d	0.27
J+9	X´q	0.45
J+10	X"d = X"q	0.2
J+11	Xl	0.14
J+12	S(1.0)	0.07
J+13	S(1.2)	0.31

Figure 6.2 Model Diagram of GENROU [28]

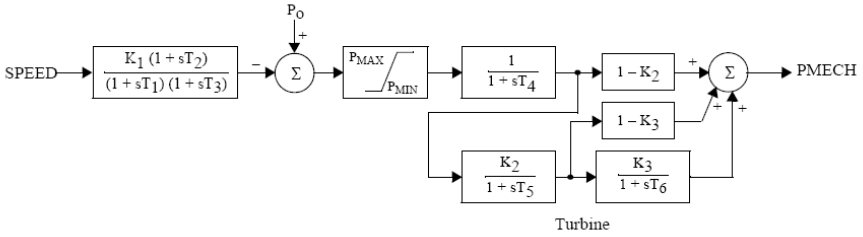

CONs	Description	Value
J	T1, controller lag (sec)	0.045
J+1	T2, controller lead compensation (sec)	0
J+2	T3, governor lag (>0) (sec)	0.2
J+3	T4, delay due to steam inlet volumes associated with steam chest and inlet piping (sec)	0.6
J+4	T5, reheater delay including hot and cold leads (sec)	0
J+5	T6, delay due to IP-LP turbine, crossover pipes, and LP end hoods (sec)	0
J+6	K1, 1/per unit regulation	22.2
J+7	K2, fraction	0
J+8	K3, fraction	0
J+9	P_{MAX}, upper power limit	1
J+10	P_{MIN}, lower power limit	0

Figure 6.3 Model Diagram of IEESGO [28]

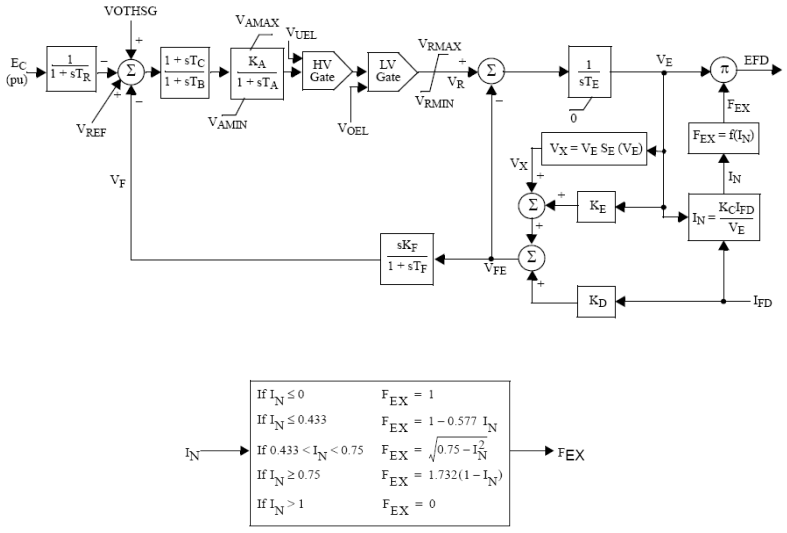

CONs	Description	Value
J	TR (sec)	0.035
J+1	TB (sec)	0.46
J+2	TC (sec)	0.26
J+3	KA	104.77
J+4	TA (sec)	0
J+5	VA_{MAX}	7
J+6	VA_{MIN}	-7
J+7	TE > 0 (sec)	0.84
J+8	KF	0.08
J+9	TF > 0 (sec)	1.5
J+10	KC	0.13
J+11	KD	0.35
J+12	KE	1
J+13	E1	1.125
J+14	SE(E1)	0
J+15	E2	1.5
J+16	SE(E2)	0.029
J+17	VR_{MAX}	7
J+18	VR_{MIN}	-7

Figure 6.4 Model Diagram of ESAC1A [28]

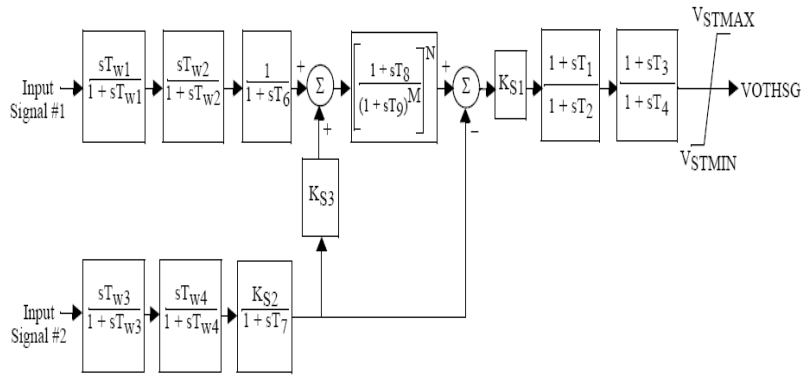

CONs	Description	Value
J	Tw1 (>0)	5
J+1	Tw2	5
J+2	T6	0
J+3	Tw3 (>0)	5
J+4	Tw4	0
J+5	T7	5
J+6	KS2	0.44
J+7	KS3	1
J+8	T8	0.5
J+9	T9 (>0)	0.1
J+10	KS1	5.2997
J+11	T1	0.515
J+12	T2	0.03
J+13	T3	0.515
J+14	T4	0.03
J+15	VST_{MAX}	0.1
J+16	VST_{MIN}	-0.1

Figure 6.5 Model Diagram of PSS2A [28]

In this test case, a shot circuit fault event, we assume three-phase-ground fault near the power plant. The event lasts 6 cycles and is cleared by tripping signal line. For the purposes of algorithm validation, it is assumed that the dynamic parameters received from the generator

owner, submitted to ERCOT, are correct. The dynamic simulation of this scenario is performed based on these existing dynamic parameters. The simulation results (Meas_P , Meas_Q, Meas_Angle, and Meas_Voltage) at bus # 8126 are treated as the PMU “measurement” data, as shown in Figure 6.6 and Figure 6.7. After that, these parameters are assumed to be unknown and are altered to some other values. The system response from these altered parameters is treated as “simulation” results. The proposed method will use the ”measurement” data to adjust these altered parameters back to the existing value, which is defined as the ”actual response value” for the proposed parameter identification process.

The algorithm is programmed in Python 2.5 with PSS/E simulation engine (version 32) and runs on a computer with Intel Core i3 Quad-Core CPU 2.27GHz and 4 GB RAM.

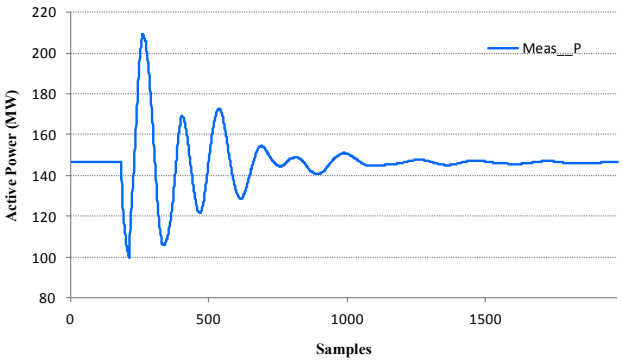

(a)

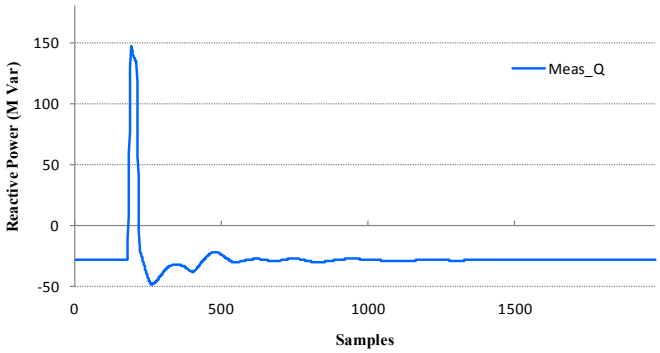

(b)

Figure 6.6 PMU Measurements at Boundary Bus (a) Active Power (b) Reactive Power

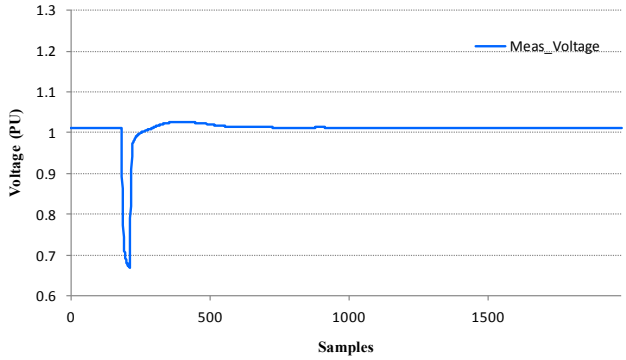

(a)

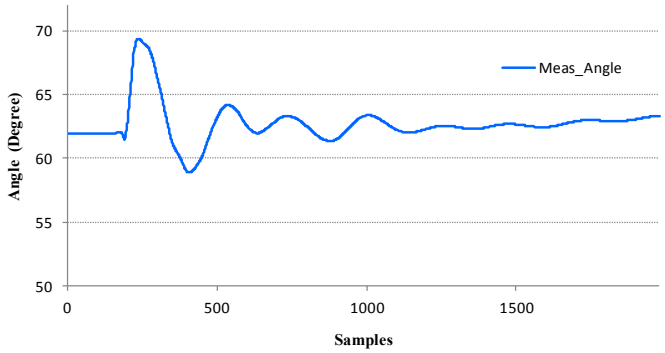

(b)

Figure 6.7 PMU Measurements at Boundary Bus (a) Voltage (b) Angle

6.2 Parameter Identification Process and Objective Function Description

6.2.1 Parameter Identification Process

The proposed implementation scheme of PMUs-based dynamic model parameter identification is shown in Figure 6.8. Firstly, the PMU data including voltage, angle/frequency, real power and reactive power – (V, δ / f , P, Q) is needed for this application. Secondly, an isolated subsystem based on measurement points of PMU must be created. The power flow case of this subsystem as shown in Figure 6.1 should match the pre-disturbance condition.

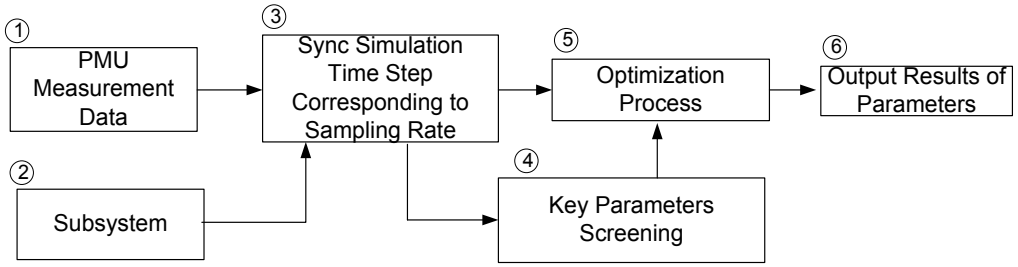

Figure 6.8 Flow Chart of Parameter Identification Process

Thirdly, in order to compare the simulation results with the actual records, the simulation time-step of dynamic simulation software shall be synchronized with the PMU's sampling rate. Afterward, the key parameter screening process is used to determine which parameters contributed more to the system simulation response. Finally, the SPSA-PSO cooperative algorithm will identify a set of parameters which will serve to minimize the mismatch between the simulation results and the measurement data.

6.2.2 Objective Function Description

The objective of this algorithm is to make the simulation curve match with the measurement curve by adjusting the key parameters derived in the trajectory sensitivity analysis. Nevertheless, the objective function cannot be directly formed by the "simple" means of squaring the difference between two curves: the measurement and simulation curves. This is because the mismatch caused by the hybrid dynamic simulation method may incidentally increase the error of the estimated results. In order to overcome this deficiency of the hybrid dynamic simulation, we must form the objective function by both the differences and similarities of the curves. The differences are used in steady-state and the similarities are used in dynamic-state. These both states can be detected by using edge detection method.

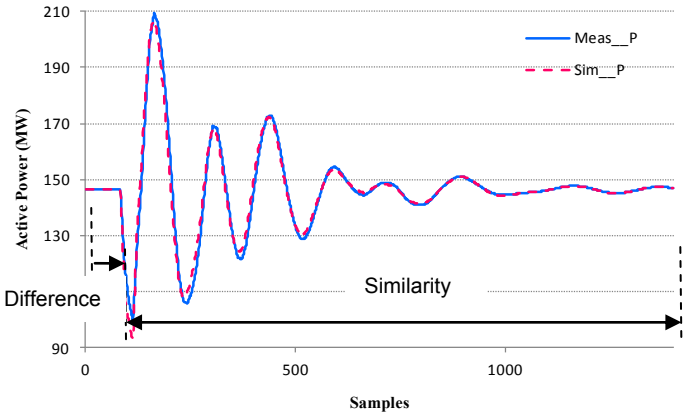

(a)

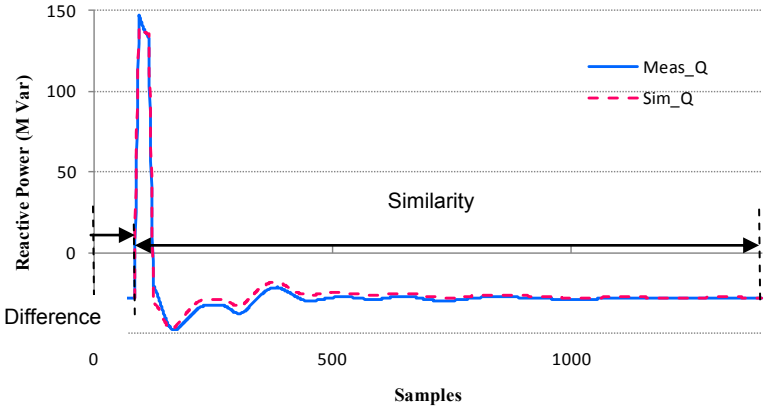

(b)

Figure 6.9 The Similarity and Difference of the Fitting Curves

This example is used to illustrate the affects of using different defined objective functions. We assumed that the fitting curves are the PMU measurement (Meas_P, Meas_Q) and hybrid dynamic simulation (Sim_P, Sim_Q) curves as shown in Figure 6.9. In the dynamic-state period, a significant mismatch between the two curves is caused by the hybrid dynamic simulation, mentioned in Chapter 3. The similarity of the waveforms defines the objective function as a squared error as in (6.1),

$$\sum_{t=1}^{n}\left(P_{meas}(t)-\mathrm{P}_{sim}(t)\right)^2 \text{ or } \sum_{t=1}^{n}\left(Q_{meas}(t)-Q_{sim}(t)\right)^2 \quad (6.1)$$

the results of MSE would be $\sum_{t=1}^{n}\left(P_{meas}(t)-\mathrm{P}_{sim}(t)\right)^2 = 8554.2$ and $\sum_{t=1}^{n}\left(Q_{meas}(t)-Q_{sim}(t)\right)^2 = 10158.0$. Since these results exhibit obvious errors, the curve fitting optimization algorithm, which is applied to find a set parameters with minimum fitness value, will fit over the curves and resulted in a set of estimated premasters with less accuracy. Therefore, in order to reduce the effects of curve mismatch, the curve similarity will be defined for forming the objective function in dynamic-state.

The problems of curve similarity appear in many applications, such as: time series analysis, shape matching, speech recognition, and signature verification, etc. Curve similarity has been studied extensively by geometer computations which can be classified as the Fréchet distance method [45]. The Fréchet distance between two curves is the similar in principle to the maximum length of a leash required to connect a dog and its owner, constrained on two separate comparison paths, as they walk without backtracking along their respective curves from one endpoint to the other. Imagine a dog walking along one curve and the dog's owner walking along the other curve, connected by a leash. Both walk continuously along their respective curve from the prescribed start point to the prescribed end point of the curve. Both may vary their speed, and even stop at arbitrary positions for various amounts of time, but neither can backtrack. The Fréchet distance between the two curves is the length of the shortest leash, not the shortest leash that is sufficient for all possible “walks,” but the shortest leash of all the leashes present, yet still being sufficient for traversing both curves in this manner. Taking the same idea of the traveling path in our application, since the comparison curves are synchronized, the similarity can be simply represented by the difference of discrete path lengths

as shown in Figure 6.10. We can determine that the greater the similarity between the two comparison cures, the closer the sum of the discrete paths.

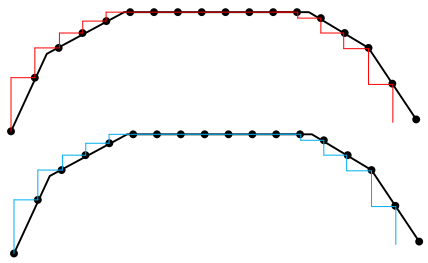

Figure 6.10 The Similarity of Two Curves Using the Discrete Path Length

Considering the curve similarity for the curves in Figure 6.8, the objective function redefined as a squared error of two discrete path lengths as in (6.2)

$$\sum_{t=1}^{n-1}\left[\left(P_{meas}(t+1)-\mathrm{P}_{meas}(t)\right)^2-\left(P_{sim}(t+1)-\mathrm{P}_{sim}(t)\right)^2\right] \quad \text{or}$$

$$\sum_{t=1}^{n-1}\left[\left(Q_{meas}(t+1)-Q_{meas}(t)\right)^2-\left(Q_{sim}(t+1)-Q_{sim}(t)\right)^2\right] \tag{6.2}$$

the values are 57.3 and 353.7 respectively. Compared with the results, 8554.2 and 10158.0, which were calculated by square error in (6.1), the objective function has been significantly improved. The estimated parameters can now be expected more precisely.

From Figure 6.9, we can note that both curves are nearly identical in steady-state, but have some mismatch in dynamic-state. In order to account for the difference in steady-state and the similarity in dynamic-state, the mathematical objective function can be formed as:

$$Min.\quad f(\lambda)=W_1\sum_{t=1}^{n}[\left(P_{meas}(t)-\mathrm{P}_{sim}(\lambda_p,t)\right)^2]+W_2\sum_{t=1}^{n}[\left(Q_{meas}(t)-Q_{sim}(\lambda_p,t)\right)^2]+$$

$$W_3\sum_{t=n+1}^{N}[\left(P_{meas}(t+1)-P_{meas}(t)\right)^2-\left(\mathrm{P}_{sim}(\lambda_p,t+1)-\mathrm{P}_{sim}(\lambda_p,t)\right)^2]+ \tag{6.3}$$

$$W_4 \sum_{t=n+1}^{N} [(Q_{meas}(t+1) - Q_{meas}(t))^2 - (Q_{sim}(\lambda_p, t+1) - Q_{sim}(\lambda_p, t))^2]$$

where

W is a weighting constant, $\sum W_i = 1$

P_{meas} and Q_{meas} are PMU measurements.

P_{sim} and Q_{sim} are simulation results.

t from *1* to n samples are in steady-state

from *n+1* to N samples are in dynamic-state

p are the most sensitive parameters based on the trajectory sensitivity analysis.

In (6.3), the first two terms in the summation, $W_1 \sum[\bullet$ and $W_2 \sum[\bullet$, represented by the difference of two curves in steady state. The similarities of the curves in dynamic state are represented by the last two terms in the summation, $W_3 \sum[\bullet$ and $W_4 \sum[\bullet$. Using the similarity in (6.3), the effects of mismatch caused by the hybrid dynamic simulation can be significantly reduced.

This dissertation forms an objective function by using waveform similarity and difference to overcome the drawbacks of the simulation mismatch. However, this multi-objective optimization problem consists of four different objectives in (6.3) which may conflict with each other, but need to achieve minimum value simultaneously. One common way to approach this problem is to find the multiple Pareto optimal solutions (Pareto front) [46] [37]. However, finding several passable solutions to build the Pareto front is even less efficient than single objective function problems. A more simple way to approach this problem is aggregating the multiple objectives into one objective function, which considering weights that can be fixed or dynamically changed during the optimization process. The main disadvantage of this approach

is the fact that it is not always possible to find the appropriate weighted functions. Fortunately, it is relatively simple to consider the constant weighting value in (6.3), because the similarity values are always remain about two to three times lower than the given difference value. More intuition inputs often include choosing $W_1 = W_2 = 0.1$ and $W_3 = W_4 = 0.4$. Afterward, the experience test results show the objective function can accurately represent the best fitness curves.

6.3 Parallel Computation

Thousands of buses and hundreds of generators exist in the EROCT system. Dynamic simulation of the ERCOT system involves the computation of thousands of algebraic and differential equations. Typically, it takes approximately one minute to perform one dynamic simulation of the ERCOT system using a desktop PC. Fortunately, the hybrid dynamic simulation can effetely reduce the size of the given subsystem, and only the models of the generator equipment residing inside this subsystem needs to be considered. However, the dynamic simulation process still requires approximately four to five seconds in order to perform a single simulation. Thanks to parallel computing technology, many results of dynamic simulation can be carried out simultaneously for accelerating the parameter identification task.

According to the level at which the hardware supports parallel computing, the multi-core and multi-processor computers having multiple processing elements within an individual machine; the clusters, the massively parallel computer (MPPs), and the grids use multiple computers to work on the same task. Specialized parallel computer architectures are sometimes used alongside traditional processors. However, parallel computer programs are typically more difficult to write than sequential ones, because concurrency introduces several new classes of potential software bugs, of which race conditions are known to be the most

common. Communication and synchronization between the different subtasks typically become some of the greatest difficulties in getting good parallel program performance.

An open source software package, Parallel Python PP [47], provides a high level interface for executing Python code in parallel on multi-core CPUs cluster. The Client is used in top-level code to submit tasks to the controller, supercomputers, and the cloud. The proposed SPSA-PSO cooperative algorithm significantly benefits from the multi-core parallel computing, because of the PSO's population-based nature as well as its concurrent objective function estimation needs of SPSA. The test cases show the benefits below. The computation time of whole process included 3,000 fitness function estimations can be cut down to 40 to 50 percent. It drastically accelerating the computation speed.

Table 6.1 The Computation Time With 3000 Fitness Function Estimations

Without parallel computing	With parallel computing
4:11:14	2:18:04

6.4 Setting of Algorithm's Parameter

Like other stochastic approximation algorithms, the proposed PSO and the 2SPSA cooperative algorithm have some parameters necessary to be chosen by the user. It is an important task to see that these parameters are selected in order to optimize the performance of the convergence and variability of the search area.

The parameters for PSO are particle numbers, inertia weight (w), the acceleration coefficients (c_1, c_2). The more particle numbers, the larger searching space which can be covered per iteration. However, having more particles increases the per iteration computational cost. It has been shown in a number of empirical studies that the PSO has ability to find optimal solutions with swarm size from 10 to 30 [48]. Since the proposed algorithm cooperated with

2SPSA, the PSO is better to have a varied searching space, therefore increasing the rate of successful solutions found. Therefore, the swarm size equal to 30 was chosen in this application. The inertia weight, w, controls the momentum of the particle by weighting the contribution of the previously recored velocity. The value of w is important to ensure convergent behavior and to optimally tradeoff between global searching ability and convergence rate. A large value of w speeds up exploration and increases diversity; while a small value of w promotes convergence at local optimal. However, the optimal value for the inertia weight is the problem dependent. The approaches with dynamic inertia weight can be classified into the four categories: random adjustment, linear decreasing, nonlinear decreasing, and fuzzy adaptive inertia [37]. A simple and efficient inertia weight adopted in this dissertation is a linear decreasing weighting as mentioned in section 5.1. The decreasing sequence descends linearly from an initially maximum inertia weight ($w_{\max}$), and ends at a minimum value, ($w_{\min}$). The values are usually set as 0.9 and 0.4 respectively. The acceleration coefficients (c_1, c_2) control the influence of cognitive and social components on the overall velocity of a particle. When c_1 and c_2 coexist in a good balance, i.e. $c_1 \approx c_2$, particles draw their moving force from their cooperative nature and are considered to be effective. Low values for c_1 and c_2 result in smooth particle trajectories, giving the particles the ability to move to far-off areas. High values cause more acceleration with abrupt movement towards or past the “good” regions. Typically, the optimized c_1 and c_2 are found empirically and through tests. In general, $c_1 = c_2 = 1.49$ can result in more stable results.

The parameters for 2SPSA are two constants (α, γ) for gain sequences (a_k and c_k), and two perturbation sizes (c and $\tilde{c}$). The choice of the gain sequences is critical to the performance of 2SPSA. With α and γ as specified in (5.6) and (5.11), we can note that

choosing $\alpha < 1.0$ yields better finite-sample performance through maintaining a larger step size; hence the recommendation to use values: 0.602 and 0.101, which are effectively the lowest allowable satisfying the theoretical conditions [42]. According to an empirically rule, it is effective to set c at a level approximately equal to the standard deviation of the measurement noise in $y(\lambda)$ in order to keep the p elements of $\hat{g}_k(\hat{\lambda}_k)$ from getting excessively large in magnitude (the standard deviation can be estimated by collecting several $y(\lambda)$ values at the initial guess $\hat{\lambda}_k$. However, a precise estimate is not required in practice. In this dissertation's application, the noise of $y(\lambda)$ only comes from minor imperfect measurements of $L(\lambda)$, then c should be chosen as some small positive value. The values of a and A can be chosen together to ensure effective practical performance of the algorithm. A large a may enhance performance in the later iterations by producing a larger step size when the effect of A is small. A guideline recommended by [42] is used to take 10% (or less) of the maximum number of allowed iterations and choose a such that $a/(A+1)^{\alpha}$ times the magnitude of elements in $\hat{g}_0(\hat{\lambda}_0)$ is approximately equal to the smallest of desired change magnitudes among the given elements of λ in the early iterations. For example, if the elements of λ typically move by a magnitude 0.1 in the early iterations, the elements in $\hat{g}_0(\hat{\lambda}_0)$ is approximately 10, then with A=100 and α =0.602, a =0.16 would be chosen. For 2SPSA, since it can achieve a nearly optimal solution with a trivial gain sequence ($\bar{a}_k = 1/(k+1)$), the difficulty of selecting *A* and a can be eliminated.

Moreover, since the scale of the generator unit's parameter varies widely, a parameter normalization process is necessary to acquire a better result. In this case, the normalization scale is 1000. The parameters used in the optimization program are shown in Table 6.2. In this study, the objective is to evaluate whether the algorithm can found the best solution within a restricted time period. A stopping condition has been used to terminate the program when a

maximum number of fitness estimations has been exceeded. In this study case, the maximum number of fitness estimations is 3000.

Table 6.2 Parameters Using In Optimization Program

PSO				2SPSA				
Particles	c1=c2	w_{min}	w_{max}	Scale	c		γ	α
30	1.49	0.2	0.9	1000	20	30	0.1667	1

6.5 Results of Dynamic Parameter Identification

To examine the effectiveness and convergence speed of the proposed SPSA-PSO cooperative method and to avoid any misinterpretation of the optimization results, we compare these results with the basic PSO by performing each method for 50 runs. Every test is started from a randomly selected initial solution and uses the same termination criteria. The termination criterion allows for 3000 evaluations of the objective function.

Table 6.3 lists the results of 50 runs. Maximum and minimum values are shown, as well as the mean values and standard deviation which were calculated. Comparison of the result of the SPSA-PSO cooperative algorithm and the results of basic PSO algorithm demonstrates that the former has performed consistently better than the latter. The convergence behaviors of the fitness values averaged by 50 runs for the two approaches are shown in Figure 6.11. It is also shown that the efficiency and accuracy has been significantly improved by using the SPSA-PSO cooperative algorithm.

Table 6.3 Statistical Results from 50 Runs

Basic PSO				Cooperative SPSA-PSO			
Max.	Min.	Mean	standard deviation	Max.	Min.	Mean	standard deviation
4.5567	1.4407	2.3334	0.7253	2.2483	1.4439	1.7734	0.1956

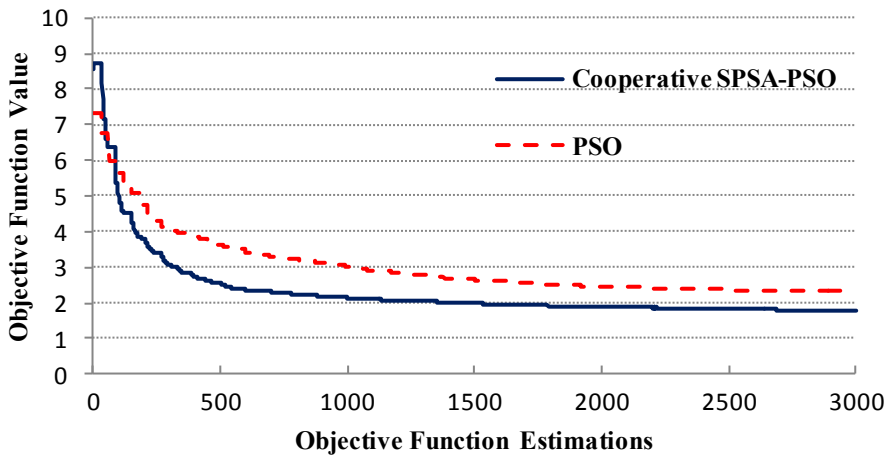

Figure 6.11 Convergence Diagram of Two Approaches

The best fitting simulation results of SPSA-PSO cooperative method among the 50 runs are shown in Figure 6.12 and 6.13. Both active power and reactive power can be fitted to be nearly identical.

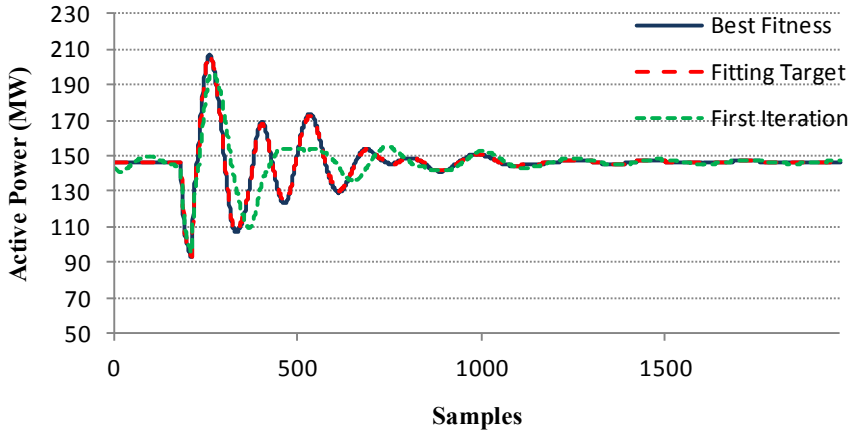

Figure 6.12 Active Power Simulation Result of Best Fitness among 50 Runs

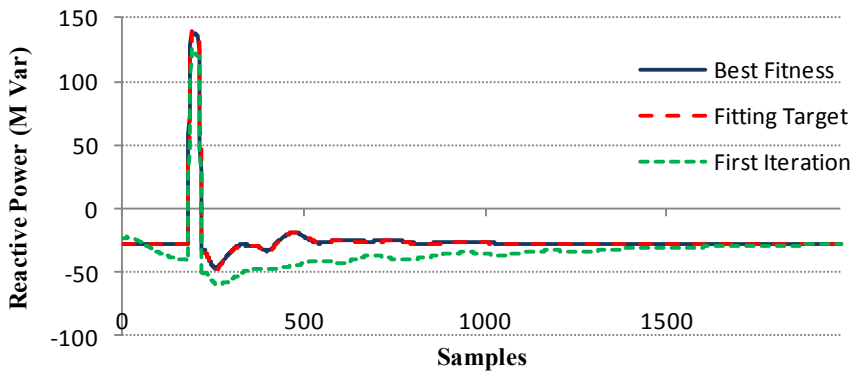

Figure 6.13 Reactive Power Simulation Result of Best Fitness among 50 Runs

The statistical results of all parameters of 50 runs of the SPSA-PSO cooperative method are shown in Table 6.4, which includes the parameter's actual value, maximum value, standard deviation (σ), mean value (μ), percentage error (ε), and the set of the best fit parameters. There are two different percentage errors; the first one (ε) is the error between the mean value and the actual value, whereas the second one (ε') represents the error between the best fit value and the actual value. We can note that the error (ε') shown in the last column of Table 6.4 is significant even if the best fit curve matches the target curve very well, as shown in Figure 6.11. The result is not surprising, because an extreme parameter correlation often hampers the calibration of a generator unit's model. Parameter correlation causing non-unique parameter values is a common problem for system identification. Regardless of how models are calibrated, the system's extreme correlation existence makes it impossible to uniquely estimate the parameters of a generator unit. This weakness could be remedied when more associated statistics are available. Therefore, taking the mean value (μ) of the parameters derived from 50 runs into account as the final estimate result becomes more accurate than the result derived

from solely the best fit result. Furthermore, the errors (ε) of the mean values are all within a small range, verifying that the results are trustworthy and reliable.

Table 6.4 The Statistic Results of Parameters through 50 Runs

Parameter	Actual	Max.	Min.	standard deviation	Mean value	percentage error	Best Value	percentage error
Generator Model -GENROU								
T´do	**8.4**	10.92	5.88	1.61	**8.63**	*2.8*	**9.28**	*10.4*
T”qo	**0.15**	0.20	0.11	0.03	**0.15**	*2.6*	**0.18**	*20.5*
H, Inertia	**4.47**	5.13	4.05	0.24	**4.58**	*2.4*	**4.73**	*5.8*
Xd	**1.98**	2.47	1.45	0.26	**2.02**	*2.0*	**1.79**	*9.7*
Xq	**1.88**	2.34	1.48	0.19	**1.92**	*2.2*	**1.61**	*14.1*
X´d	**0.27**	0.32	0.23	0.02	**0.27**	*0.7*	**0.27**	*0.0*
X´q	**0.45**	0.49	0.41	0.03	**0.45**	*0.1*	**0.46**	*2.2*
X”d= X”q	**0.2**	0.24	0.16	0.02	**0.20**	*0.8*	**0.20**	*0.4*
Xl	**0.14**	0.18	0.10	0.02	**0.14**	*2.1*	**0.13**	*9.2*
Exciter Model- ESAC1A								
T7	**5**	6.50	3.57	0.80	**4.87**	*2.6*	**4.66**	*6.8*
KS2	**0.44**	0.56	0.32	0.06	**0.45**	*1.9*	**0.44**	*0.3*
KS3	**1**	1.30	0.71	0.17	**1.04**	*3.6*	**1.09**	*9.1*
T9 (>0)	**0.1**	0.13	0.07	0.02	**0.10**	*2.9*	**0.12**	*22.8*
Power System Stabilizer Model-PSS2A								
TB (sec)	**0.46**	0.60	0.32	0.07	**0.45**	*2.8*	**0.50**	*9.5*
TC (sec)	**0.26**	0.34	0.19	0.04	**0.26**	*1.8*	**0.31**	*18.5*
KA	**104.8**	136.20	80.34	12.82	**107.44**	*2.6*	**104.76**	*0.0*
TE (sec)	**0.84**	1.06	0.62	0.12	**0.84**	*0.1*	**0.81**	*3.1*
KF	**0.08**	0.10	0.06	0.01	**0.08**	*1.3*	**0.07**	*11.3*
KD	**0.35**	0.45	0.25	0.06	**0.36**	*2.4*	**0.37**	*6.4*
KE	**1**	1.27	0.70	0.15	**1.01**	*0.5*	**1.07**	*7.4*

6.6 Summary

A new SPSA-PSO cooperative algorithm and a novel parameter identification scheme are discussed in this dissertation. The new algorithm and scheme are used to evaluate the parameters of dynamic models from PMU-based measurements recorded during disturbances.

The SPSA-PSO cooperative algorithm is used to estimate power system parameters from measurements taken during a system disturbance. The algorithm is based on PSO and 2SPSA method, in which the 2SPSA provides a more efficient way to improve the global best position and accelerate convergence. This reliable algorithm significantly improves the global search ability and convergence rate.

Using hybrid dynamic simulation, the system outside the studied model can be effectively reduced. Therefore, the quality of the results and the computation time are dramatically improved. Moreover, trajectory sensitivities provide information which is valuable for determining key parameters. This dissertation establishes a close link among hybrid dynamic simulation, trajectory sensitivity, and the optimization algorithm for parameter identification processes.

The proposed approach has been demonstrated in a case that models a newly installed generator unit in the ERCOT system. This approach is proven to have superior features, including high accuracy of the estimated results, stable convergence, and good computational efficiency. The most important features of the proposed approach are feasibility, simplicity, and relatively ease of implementation for an ISO.

CHAPTER 7

CONCLUSIONS AND FUTURE RESEARCH

7.1 Conclusions

The accuracy of the dynamic parameters affects the reputation of the power system dynamic simulation, thereby affecting the economical implications and overall reliability of the power system. Inaccurate dynamic simulation results may lead to exceedingly conservative estimation of the system transfer limit, such as TTC, or ATC, causing additional congestion in the power market. Additionally, this factor will singlehandedly increase the market clearing price (MCP) or locational marginal price (LMP) and decrease the utilization rate of the transmission network. Alternatively, inaccurate dynamic simulation results could lead to overestimation of the system transfer limit, as well. In the worst case scenario, this may give rise to a local or system level blackout. Therefore, it is very important to ensure the accuracy of the dynamic parameters in the system database for simulation. However, the mismatch between simulation results and the on-site recording data exists as documented data in research papers and reports of fault-event investigation. The area of dynamic parameter estimation is thus being identified as a potential area of research by the engineers and researchers in the power system area.

The current methods of online dynamic parameter estimation for generator unit typically depend upon the given on-site measurements, such as field current, voltage, and rotor speed. From ISO's implementation point of view, it is difficult or even impossible to access necessary measurement records. Meanwhile, PMUs have been widely installed nationwide, and the approach of PMU-based dynamic parameter estimation continues to gain momentum as a prominent solution for the utility industry to reach the goal of total parameter verification and identification automatically. For that reason, this dissertation proposes an identification process

in order to demonstrate and prove that PMU-based dynamic parameter estimation is a feasible solution for the discussed issues.

The predominant issues, tremendous computation time and initial guess solution, are two troublesome obstacles for the optimization algorithm of parameter identification processes. The approach proposed in this dissertation is described as a robust method for accurate dynamic parameter estimation. The proposed method utilizes a new intelligent method, PSO, to find the global optimization solutions and uses a second-order gradient-based method, 2SPSA, to speed up the convergence rate of PSO. The initial guess solution for PSO is no longer required and has an outstanding global searching ability. Meanwhile, the slow convergence rate of PSO is vastly improved by 2SPSA. Therefore, the proposed method could keep the balance of global searching ability and convergence rate. Additionally, the optimization algorithm is programmed with parallel calculating structure to take advantage of the multi-core computer to reduce computation times.

The proposed method achieves the target value of the dynamic parameters such as generators, governors, exciters, and PSS in the assumed test case. It successfully tunes each of the dynamic parameters of the generator, governors, exciter, and PSS in a given power plant to dramatically decrease the mismatch between the simulation results and the field recording data following the disturbance event in ERCOT system.

7.2 Possible Future Research

7.2.1 Future works

The research presented a test case to demonstrate and verify the proposed parameter identification process. The results show that the proposed approach can be a promising solution for solving PMU based parameter identification problems. There are several future works stemming from this work which could be pursued to improve the accuracy of estimation results and to deal with reality application issues.

- Use a statistical analysis approach, such as the parameter regression method to remediate the affect of parameter correlation.
- Decouple the identification model to increase the accuracy of estimated results. For example, the governor model and d-axis parameters of generator can only matching with P (active power) measurement; the exciter model and q-axis parameters of generator can only matching with Q (reactive power) measurement.
- Use several results derived from different disturbance events to accurately determine a set of parameters.
- Develop a user-friendly interface to reduce the complexity of program usage.
- Develop an automatic data retrieving process for assessing disturbance records from PMUs, as well as the pre-disturbance power flow case from EMS.
- Design a signal denoising filter for the disturbance records, if the signals are accompanied by noise.

7.2.2 Potential Research

The current installed wind generation capacity in Texas is more than 10,000MW, which accounts for about 10% of the total installed generation capacity in ERCOT. In the near future, the overall wind generation in ERCOT will be approximately one third of the total installed generation capacity. The potential stability problems caused by the wind farms should be considered important to ERCOT. Therefore, it is virtually necessary to conduct the dynamic study, including frequency and voltage stability. The voltage stability results are highly affected by the dynamic load model in the system. However, dynamic simulations using standard static stability load models were not successful in reproducing the event. The actual response of the transmission system may be reproduced using aggregate load models that include the effect of induction motors and distribution system impedances. Therefore, it is critical that the load

models used in dynamic studies correctly represent the behavior of actual load. As noted, there is no dynamic load model in the current model database in ERCOT. It is very urgent to develop a dynamic load model to prevent associated phenomenon, such as fault induced delayed voltage recovery, which may result in a large amount of load loss, as previously experienced in WECC.

Although this dissertation focuses on the generator, exciter, governor, and PSS parameters, the proposed method can be extended to any other dynamic method, such as load models and wind generator models, since they are model-independent methods. Meanwhile, this approach opens doors to similar opportunities, such as:

- Indentifying the wind-turbine or big-size motor's parameters and monitoring the health conditions.
- Detecting the power system areas which exist in simulation mismatch validation.
- Identifying the dynamic load model.
- Calibrating the parameters of a transmission line or transformer.
- Validating the power system simulation software.

As mentioned in the introductory chapter, the model/parameter validation is a long-term and on-going effort. The proposed approach should be automatically invoked following any form of disturbance event. Following the disturbance events, the pre-disturbance power flow case from SCADA/EMS and the disturbance PMU measurement data could be sent to the computer where the proposed application is located. The proposed method would then use the captured data to validate the simulation results and determine the mismatched areas which PMU measurements have significant differences with the simulation results. After the inaccuracy models have been located, parameters in the model database will begin the calibration processes. The optimized parameters will then be recommended by the program to decrease

the discrepancy when the mismatch index is high. The basic system infrastructure required for the application of the proposed method is shown in Figure 7.1.

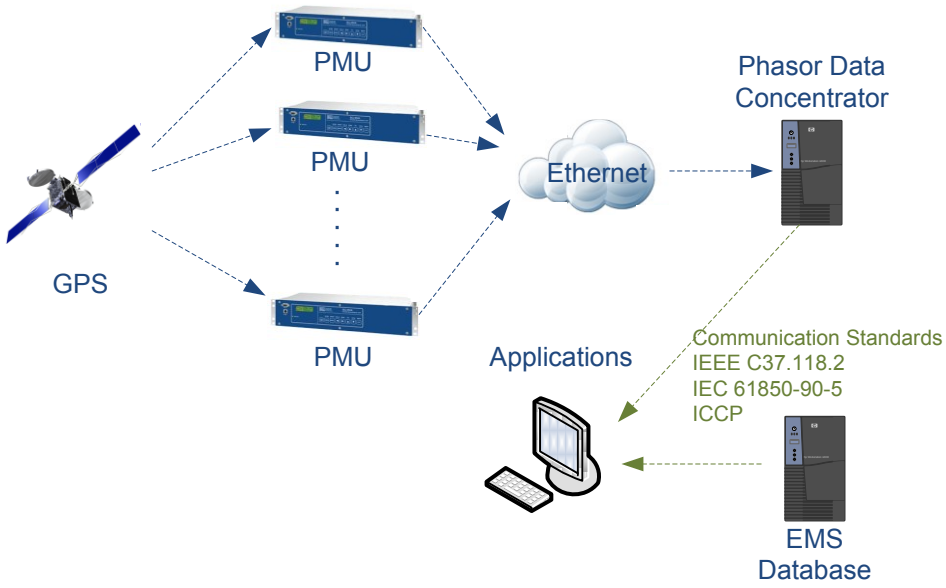

Figure 7.1 Basic System Structure of Proposed Application in Parameter Identification

The most commonly used communication standards as shown in Figure 7.1 are IEEE C37.118.2, IEC 61850, or ICCP [21]. These protocols can run over TCP/IP networks and/or substation LANs using high speed Ethernet to obtain the necessary response times of < 4 ms for data communication. Currently, C37.118 is widely used for synchrophasors and is adequate for many systems. In order to adapt to IEC, C37.118 split into separate standards, the new standard, C37.118.2, covers only the communications for measurement; IEC 61850 is new development for synchrophasors communications and other substation automation, and ICCP is defined to provide a communication profile for sending basic telecontrol messages between two systems, and is often widely used in EMS or substation communication. As a system uses more than one kind of communication standards, the issue of protocol harmonization and integration will become more important for the application of the proposed method.

Recently, the Electrical Power Research Institute (EPRI) conducted a study of the CIM (Common Information Model) for power system dynamic models. The electric utility software vendors are encouraged to exchange XML (Extensible Markup Language) versions of the CIM to demonstrate interoperability of products. Including CIM in the loop will enhance the capability of the proposed parameter estimation process.

7.2.3 Potential Applications

While the proposed approach, the dynamic parameters estimation for generation facilities, has been implemented in ERCOT, the system models can attain an even better calibration level. Furthermore, the hardware installation as shown in Figure 7.1 would also satisfy the need of a “smart grid” which employs innovative technologies and services, coupled with intelligent monitoring, control, communication, and self-healing applications; the software utilized in this dissertation could also be applied to realize the essential calculation of the smart grid. All technology areas could deploy on a fully optimized electricity smart grid as shown in Figure 7.2. However, the applications discussed here focus on transmission level, and not all technology areas are suitable for this application. Based on the proposed hardware structure, the potation applications are as following:

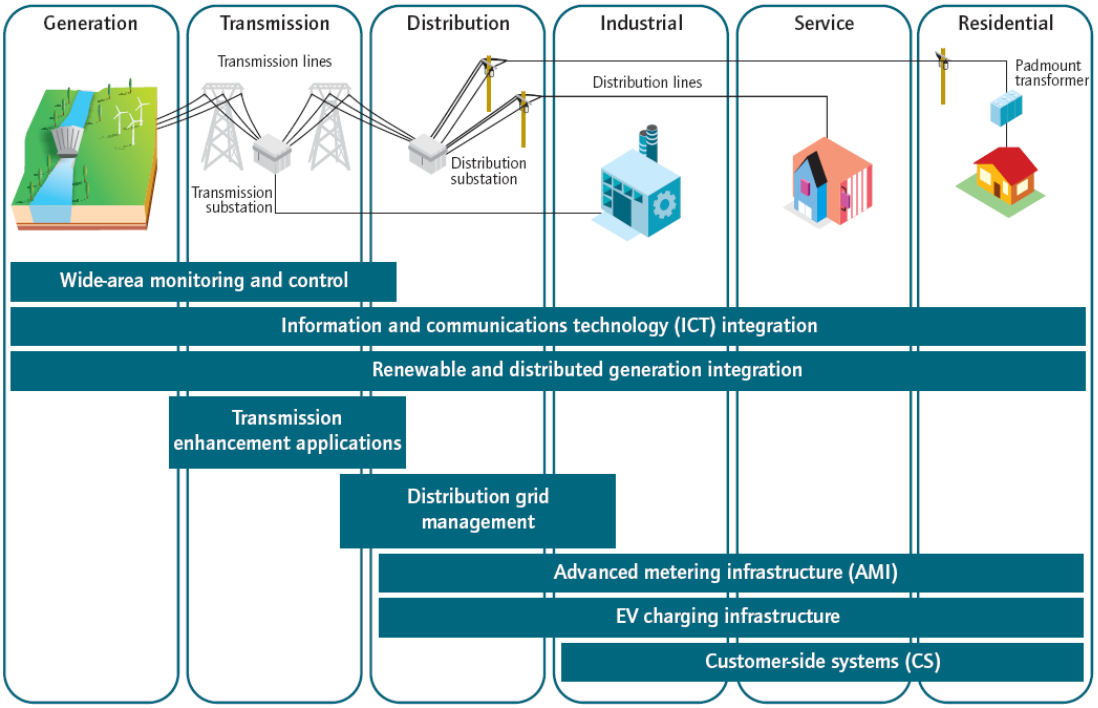

Figure 7.2 Smart Grid Technology Areas [49]

- Wide-area monitoring and control

Real-time monitoring and display of power system components and performance, across interconnections and over large geographic areas, help system operators to understand and optimize power system components, behavior, and performance. Advanced system operation tools avoid blackouts and facilitate the integration of various renewable energy resources. Monitoring and control technologies along with advanced system analytics – including wide-area situational awareness (WASA), wide-area monitoring systems (WAMS), and wide-area adaptive protection, control and automation (WAAPCA) – generate data to inform decision making, mitigate wide-area disturbances, and improve transmission capacity and reliability.

- Renewable and distributed generation integration

It can become difficult to integrate renewable and distributed generator resources which include the large scale at the transmission level, the medium scale at the distribution level, and the small scale on commercial or residential buildings. In addition, energy storage systems can alleviate some operation problems by decoupling the production and delivery of energy. The problems of dispatch and control upon these resources to power system become even more complicated. The proposed structure can help through automating the control of generation and demand to ensure an optimized balance of supply and demand.

- Transmission enhancement applications

There are a number of technologies and applications for the transmission system. Flexible AC transmission systems (FACTS) could are used to enhance the controllability of transmission networks and maximize power transfer capability. The deployment of this technology on existing lines can improve efficiency and defer the need of additional capital investment. High voltage DC (HVDC) technologies are used to connect wind farms, solar farms, and inter-area to power system, with decreased system losses and enhanced system controllability, allowing efficient use of energy sources, despite being operated from remote load centers. Dynamic line rating (DLR), which uses sensors or weather data to identify the current carrying capability of transmission lines in real time, can optimize the utilization of existing transmission assets, without the risk of causing overloads. The proposed structure can help to enhance the utility of those facilities in order to improve the stability and reliability of entire electric system.

APPENDIX

USER INSTROCTIONS OF PARAMETER IDENTIFICATIO PROCESS

Software Requirement

- PSS/E 32 Version
- Python 2.5 Version
- NumPy / SciPy – are two of many open-source packages for scientific computation used the Python programming language.
- Matplotlib -is a python 2D plotting library.
- Xlrd/Xlwt- are two libraries for developers to extract data or to create spreadsheet from Microsoft Excel spreadsheet files

Input Data Requirement

- An Initial Study Case:

An isolated subsystem case should be provided and the all boundary buses of his subsystem should have PMU installed or synchronized data are available.

- A PMU measurement data:

The disturbance record, real power P, reactive power Q and Bus Voltage and Angle, are the minimum requirement. The length of recorded data is at least 10 seconds and the sampling rate should be higher than 20Hz.

Step-by-Step Usage Instruction

This appendix contains the step-by-step procedures for generator parameter identification process for example case in Chapter 6. Each step of this section documents a single necessary activity for parameter identification process.

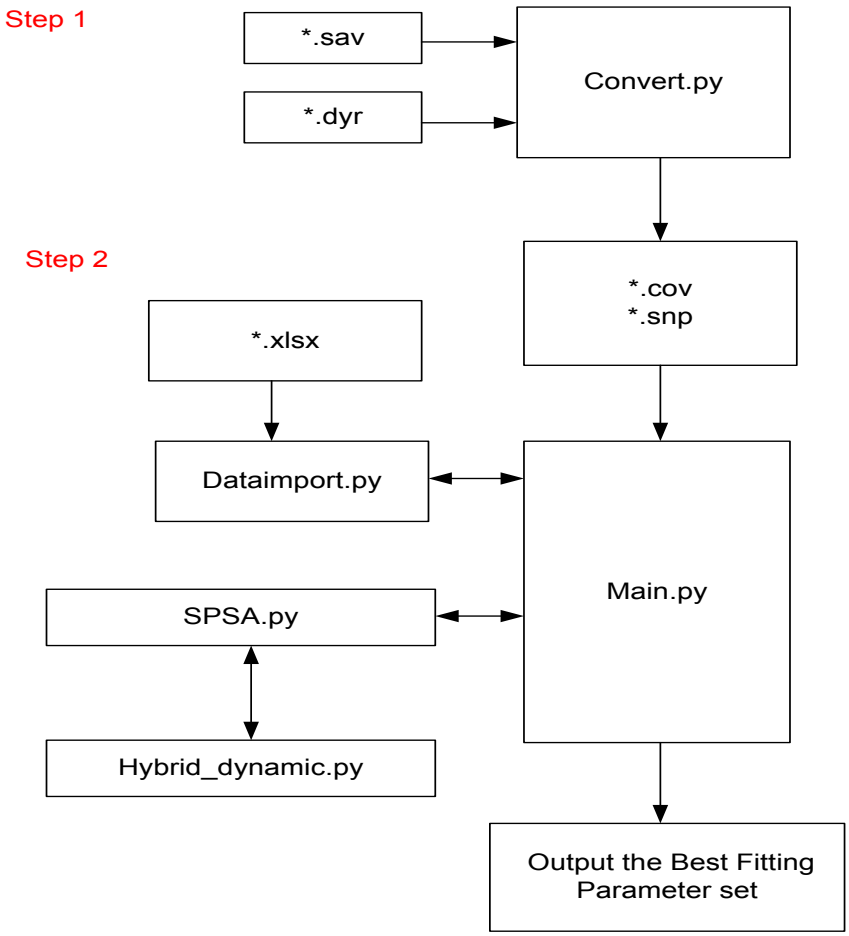

Figure A.1 Block Diagram of the Program

Two steps process are designed to accomplish the unit's parameters identification. As shown in Figure A.1, in the first step, *Convert.py* is used to convert power flow case *(*.sav)* and

link dynamic model file *(*.dyr)* into a converted file *(*.cov).* Meanwhile, the snapshot file *(*.snp)* also will be created.

The second step is the *Main.py* which used to import the measurement data *(*.xlsx)* and run the optimization process, *SPSA.py*, to find a best fitting parameters set. To improve simulation accuracy and reduced the complexity of simulation case, the *Hybrid_dynamic.py* is developed for this proposed.

Input Data

The input data is the record data of PMU saved in EXCEL spreadsheet format. As shown in Figure A.2, the first column is time stamp where time value should begin from 0 second to the length of data record and the sapling rate of data is recommended higher than 20 Hz. The measurement data should include voltage amplitude, voltage angle, real power and reactive power the unit of that values are p.u., degree, MW and Mvar respectively.

	A	B	C	D	E
9	**TIME**	**Voltage**	**Angle**	**P**	**Q**
10	0	1.011	61.968	-146.33	27.97
11	0.05	1.011	61.968	-146.33	27.971
12	0.1	1.011	61.968	-146.33	27.971
13	0.15	1.011	61.968	-146.33	27.971
14	0.2	1.011	61.969	-146.33	27.971
15	0.25	1.011	61.969	-146.32	27.97
16	0.3	1.011	61.969	-146.32	27.97
17	0.35	1.011	61.97	-146.32	27.969
18	0.4	1.011	61.97	-146.32	27.969
19	0.45	1.011	61.971	-146.32	27.968
20	0.5	1.011	61.972	-146.32	27.966
21	0.55	1.011	61.973	-146.31	27.965
22	0.6	1.011	61.975	-146.31	27.964
23	0.65	1.011	61.977	-146.31	27.962
24	0.7	1.011	61.979	-146.31	27.961
25	0.75	1.011	61.981	-146.31	27.96
26	0.8	1.011	61.983	-146.31	27.958
27	0.85	1.011	61.986	-146.31	27.957
28	0.9	1.011	61.988	-146.31	27.955
29	0.95	1.011	61.991	-146.31	27.954

Figure A.2 Input Data Format

System Reduction

As shown in below figure, an example system is created to illustrate the requirement of power flow case. Assumed the PMU is installed in Bus 8126, the network structure of internal system needs to build up as a PSS/E power flow case.

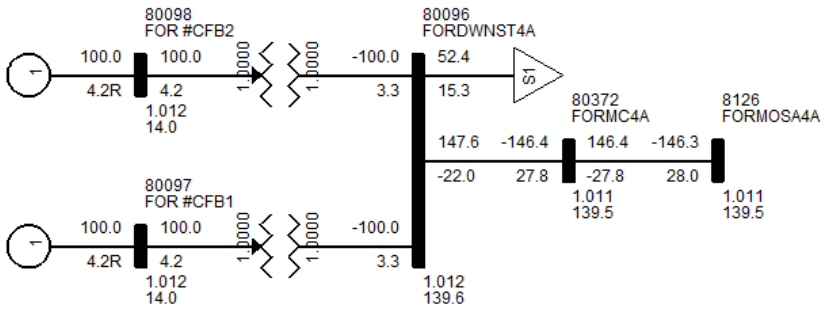

Figure A.3 An Internal System from Measurement Point

From measurement point, bus 8126, a transformer and a generator need to add in.

Since the impedance of the transformer is not zero, negative impedance is connected between transformer and generator to cancel the mismatch caused by this impedance. The network configure is shown in Figure A.4.

Based on the system condition in steady state before disturbance, the users can adjust the power flow of this reduction system which is identical to the original system. For this case, only the P and voltage of generators need to adjust. Finally, the power flow case of this complete reduced system saves into a **.sav* file.

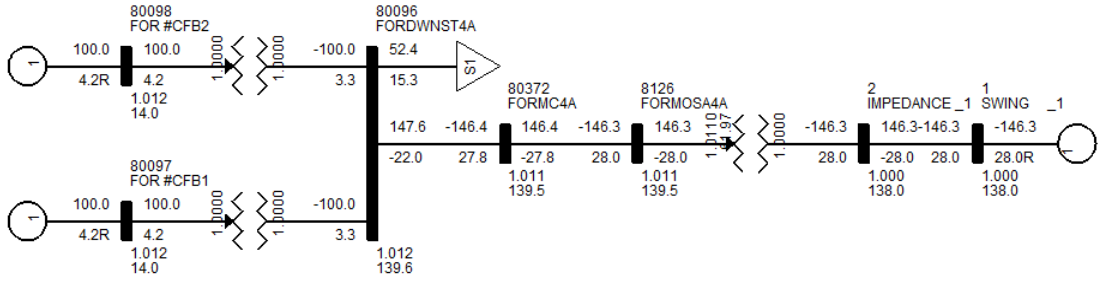

Figure A.4 the Complete Reduced System

Environment Setting

All of files, measurement data, PSS/E case, should be put into the same file directory where the execution path of our developed Python program. In addition, each developed Python program in begin section has defined the path of PSS/E's python program. The user should set this path according to the directory of PSS/E installation. Where to setting this path is shown as following:

```
3  #------------------------------------------------------------------------------
4  ##set envir path
5  import os,sys
6  sys.path.append(r"C:\Program Files (x86)\PTI\PSSE32\PSSBIN")
7  os.environ['PATH'] = r"C:\Program Files (x86)\PTI\PSSE32\PSSBIN;"+ os.environ['PATH']
8
```

Figure A.5 the Setting of PSS/E Program Path

Dynamic Case Convert

The linkage and conversion of the activities DYRE, case Convert and SNAP of PSS/E is accomplished by the subroutine called *Convert.py*. The file name of power flow case *(*.sav)* and the converted case are shown as below.

```
#-----------------------------------------------
psspy.powerflowmode()
psspy.case(r"""FOR_CFB_Reduced.sav""")
psspy.conl(_i,_i,1,[0,_i],[_f,_f,_f,_f])
psspy.conl(1,1,2,[_i,_i],[0.0,0.0,100.0,100.0])
psspy.conl(_i,_i,3,[_i,_i],[_f,_f,_f,_f])
psspy.cong(0)
psspy.ordr(0)
psspy.fact()
psspy.tysl(0)
psspy.save(r"""FOR_CFB_Reduced.cov""")

```

Figure A.6 the File Name of Power Flow Case and Converted Case

The dynamic file of model *(*.dyr)* and output channel selection are shown in below figure. Where the voltage, angle, P and Q at measurement point, bus 8126, are selected.

```

psspy.dynamicsmode(0)
psspy.dyre_new([1,1,1,1],r"""CFB.dyr""",r"""cc""",r"""ct""",r"""comp""")

psspy.voltage_and_angle_channel([-1,-1,-1,8126],[])

psspy.branch_p_and_q_channel([-1,-1,-1,8126,80372],'1',[])

```

Figure A.7 the Dynamic File and Output Channel Selection

The last setting is to define the snap file *(*.snp),* shown in below.

```

psspy.snap([-1,-1,-1,-1,-1],r"""FOR_CFB_Reduced.snp""")
```

Figure A.8 the Snap File

Trajectory Sensitivity

The key parameter screening process is handled by a standalone program called *Trajectory Sensitivity.py* which is similar to *main.py* process mention in previous section. The

converted case (*.cov) , the snapshot case (*.snp) and the measurement data (*.xlsx) are necessary to give before executing the *Trajectory Sensitivity.py*

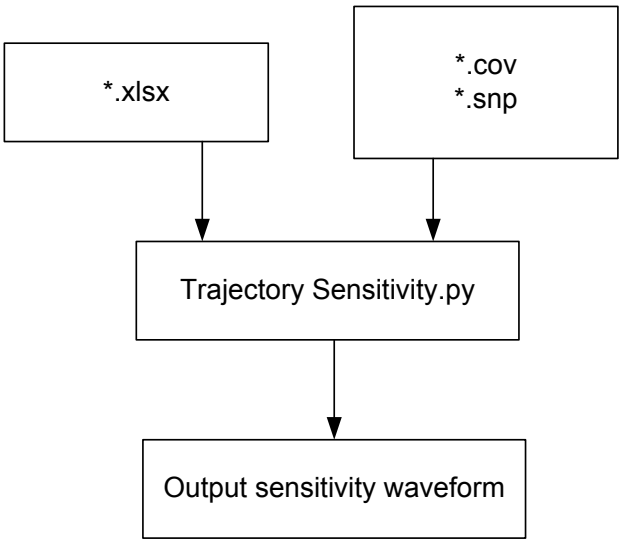

Figure A.9 the Flow Chart of Trajectory Sensitivity

As shown in below, a unit at bus 80097 is an example, where executor, generator, stabilizer and governor are defined before performing the trajectory sensitivity.

```
52  ierr, EXC_Con_Begin_Index = psspy.mdlind(80097, '1', 'EXC', 'CON')
53  ierr, EXC_Con_Number = psspy.mdlind(80097, '1', 'EXC', 'NCON')
54  ierr, GEN_Con_Begin_Index = psspy.mdlind(80097, '1', 'GEN', 'CON')
55  ierr, GEN_Con_Number = psspy.mdlind(80097, '1', 'GEN', 'NCON')
56  ierr, STAB_Con_Begin_Index = psspy.mdlind(80097, '1', 'STAB', 'CON')
57  ierr, STAB_Con_Number = psspy.mdlind(80097, '1', 'STAB', 'NCON')
58  ierr, GOV_Con_Begin_Index = psspy.mdlind(80097, '1', 'GOV', 'CON')
59  ierr, GOV_Con_Number = psspy.mdlind(80097, '1', 'GOV', 'NCON')
```

Figure A.10 the Definition of Unit's Model (for the unit at bus 80097)

In addition, the bus-id, bus-number and model's name also need to address as shown in below.

```
133    Bus_Id='1'
134    Bus_Number=80097
135
136    model_number=4      # four models
137    model_data=[]
138    model_data = [[0]*2 for i in range(0,model_number)]
139    model_data[0][0]='GENROU'
140    model_data[1][0]='IEESGO'
141    model_data[2][0]='PSS2A'
142    model_data[3][0]='ESAC1A'
```

Figure A.11 the Unit's Information (for the unit at bus 80097)

Each model with two trajectory sensitivity output, P and Q, will be provided and the MSE caused by each parameter also will be label on up right corner of output diagram. In this study case, 4 models are used; therefore, 8 trajectory sensitivity outputs are produced. The below diagram shows the two of them for example.

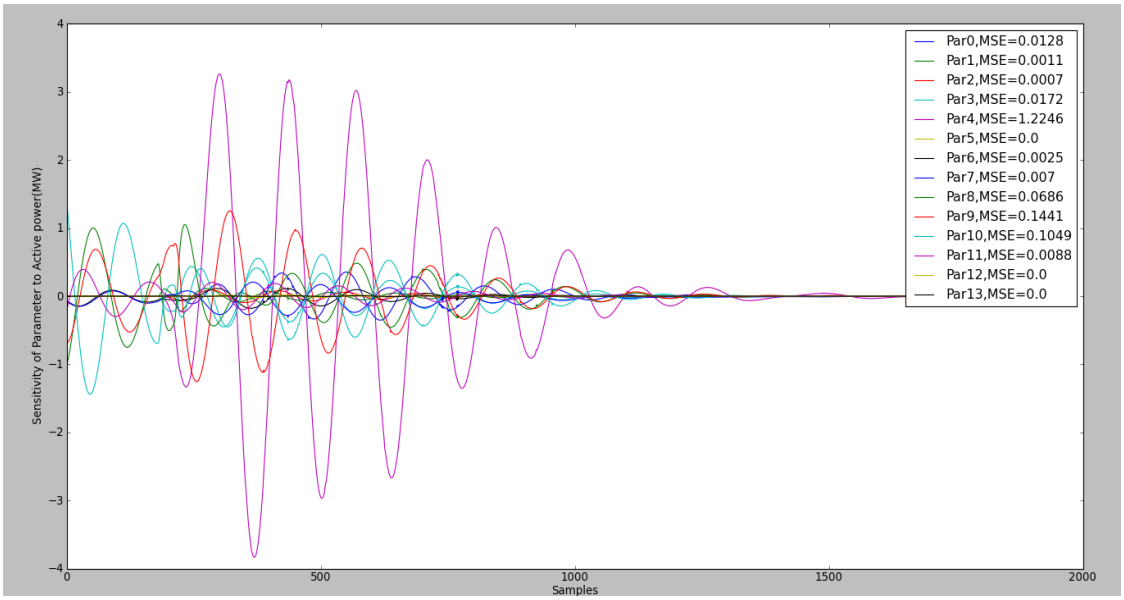

Figure A.12 Trajectory Sensitivity of Real Power (P) Corresponding to Model of Generator

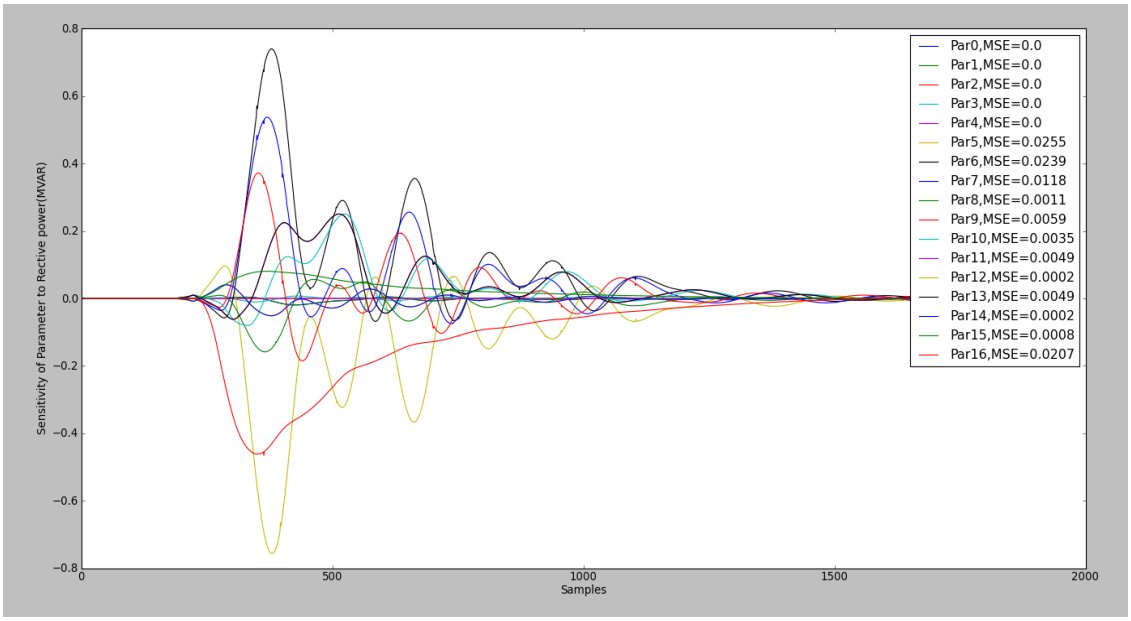

Figure A.13 Trajectory Sensitivity of Reactive Power (Q) Corresponding to Model of Exciter

Users, on above results and their own experiments, can easily choose the parameter that contributed more on output mismatch and is necessary to adjust as key parameters.

Main Program

After the key parameters are decided, the main program, main.py, is used to perform the parameters evaluation process. As mentioned before, the necessary files and relate information of identify target need to be checks before performing this process are:

converted file (*.cov)

snapshot file (*.snp)

Generator‘s model information

Index of key parameters

The place to check above data are shown sequentially in below diagrams

Converted file (.cov) and snapshot file (*.snp)*

```
psspy.rstr(r"""FOR_CFB_Reduced.snp""")
psspy.powerflowmode()
psspy.case(r"""FOR_CFB_Reduced.cov""")
```

Generator's model information

```
ierr, EXC_Con_Begin_Index = psspy.mdlind(80097, '1', 'EXC', 'CON')
ierr, EXC_Con_Number = psspy.mdlind(80097, '1', 'EXC', 'NCON')
ierr, GEN_Con_Begin_Index = psspy.mdlind(80097, '1', 'GEN', 'CON')
ierr, GEN_Con_Number = psspy.mdlind(80097, '1', 'GEN', 'NCON')
ierr, STAB_Con_Begin_Index = psspy.mdlind(80097, '1', 'STAB', 'CON')
ierr, STAB_Con_Number = psspy.mdlind(80097, '1', 'STAB', 'NCON')
ierr, GOV_Con_Begin_Index = psspy.mdlind(80097, '1', 'GOV', 'CON')
ierr, GOV_Con_Number = psspy.mdlind(80097, '1', 'GOV', 'NCON')
```

```
Bus_Id='1'
Bus_Number=80097
model_number=4     # four models
model_data=[]
model_data = [[0]*2 for i in range(0,model_number)]
model_data[0][0]='GENROU'
model_data[1][0]='IEESGO'
model_data[2][0]='PSS2A'
model_data[3][0]='ESAC1A'
```

Index of key parameters

```
para_index[0]=[0,1,2,3,4,6,7,8,9,10,11]    # Gen
para_index[1]=[0,2,3,4,6]        # Gov
para_index[2]=[5,6,7,8,9,10,11,12,13,14]    # Stab
para_index[3]=[0,1,2,3,7,8,9,10,11]  # Exc
```

Figure A.14 the Input Data for Main Program

The search range of parameters also needs to be defined; $\pm 40\%$ of parameter default value in this case is used to set up the search space.

```
        ParameterMax[x_ind]=ParameterMax[x_ind]+ParameterMax[x_ind]*0.40;
        ParameterMin[x_ind]=ParameterMin[x_ind]-ParameterMin[x_ind]*0.40;
```

Figure A.15 Setting the Hi/Low Limit of Parameters

Data Import subroutine

The subroutine, Dataimport.py, is a procedure to import data from Excel spreadsheet as following process.

```
15      num_col=5                                                    #
16      begin_row=10
17
18      import xlrd
19      workbook = xlrd.open_workbook('simulation result.xls')
20      sheet = workbook.sheet_by_name("Sheet1")
```

Figure A.16 Import File of Measurement Data

where *num_col* is the value used to define the column number of input data and *begin_row* is the first row of input data. Furthermore, the file name and spreadsheet name also need to define as shown in Figure A.16. The length of data will be detected automatically.

Optimization algorithm subroutine

The optimization used to find the best fitting parameters set is SPSA, the subroutine called *SPSA.py*. As mentioned in previous section, the some critical values of SPSA should be properly decided. They are set as following in this case. Where *Nspsa* is the maximum iteration number and the value of *a, A, alpha, gamma and c* are parameters in section5.2.

```
26      Nspsa=1000
27      Normalize_Base=1000
28
29      a=300
30      A=70
31
32      alpha=0.602
33      gamma=0.101
34      c=20
```

Figure A.17 the Parameters of SPSA

Hybrid Dynamic Simulation Subroutine

The value of measurement voltage and angle should be replaced into PSS/E when trying to implement hybrid dynamic simulation. A subroutine, *hybrid_dynamic.py*, is created to enforce the simulation initial value at each sampling step the same with the data at measurement point.

The **.snp* and **.cov* file need to read into PSS/E again and a text file for logging the information of simulation log also need to give.

```
39    psspy.rstr(r"""FOR_CFB_Reduced.snp""")
40    psspy.powerflowmode()
41    psspy.case(r"""FOR_CFB_Reduced.cov""")
42    psspy.dynamicsmode(0)
43    psspy.fact()
44    psspy.set_relang(1,-1,r"""1""")
45    #psspy.set_relang(1,Bus_Number,Bus_Id)
46    psspy.strt(0,r"""out1.out""")
```

Figure A.18 Import File of Study Case

Moreover, the two buses of inserted ideal transformer need to give as below. Where bus 8126 is measurement point and bus 2 is the bus which connected to ideal generator.

```
108    ierr,realaro = psspy.two_winding_data_3(8126,2,'1',[_i,_i,_i,_i,
109                                                        ,[_f,_f,_f,Meas_Bus_Vc

47    psspy.dynamics_solution_param_2([99,_i,_i,_i,_i,_i,_i,_i],[ 0.7,_f, 0.005,_f,_f,_f,_f,_f])
```

Figure A.19 The Bus Number of Ideal Transformer (above) and the Sampling Rate of Imported Measurement Data (below).

Output Results

Until the optimization process is finished, the final results will be saved into *Result.txt* which path is defined in *SPSA.py*.

```
23
24
```

```
Result_file = open(cur_path+"\Result.txt","w")
```

Figure A.20 Import File of Measurement Data

And the result shown the final results that contain all parameters of each model in *Result.txt* are as following.

```
Final Theta Value:
Model:'GENROU'
array([  1.14125861e+01,   3.42179744e-02,   1.61012472e+00,
         1.49587243e-01,   4.54701689e+00,  -1.56595798e-09,
         1.73096151e+00,   1.43641325e+00,   2.99068212e-01,
         4.96905192e-01,   2.32698131e-01,   1.84413342e-01,
         6.99999978e-02,   3.10000003e-01])
Model:'IEESGO'
array([  4.14212890e-02,  -2.83689909e-09,   1.20592107e-01,
         5.28767820e-01,  -5.31522270e-10,   1.64313413e-09,
         2.60865716e+01,  -1.79016263e-09,  -2.23067114e-09,
         1.00000001e+00,   2.96494151e-09])
Model:'PSS2A'
array([  5.00000000e+00,   5.00000000e+00,  -9.11126996e-10,
         5.00000000e+00,   1.68160500e-09,   4.71315190e+00,
         3.89857395e-01,   7.22539514e-01,   4.53341162e-01,
         1.11636005e-01,   7.44053013e+00,   4.04158807e-01,
         3.26200091e-02,   4.20089780e-01,   3.32489791e-02,
         1.00000002e-01,  -1.00000000e-01])
Model:'ESAC1A'
array([  2.06315374e-02,   4.44518110e-01,   3.64696172e-01,
         7.57119637e+01,   3.81383251e-09,   7.00000000e+00,
        -7.00000000e+00,   9.05823302e-01,   6.60734522e-02,
         1.33689508e+00,   1.56064245e-01,   2.89357366e-01,
         1.00000000e+00,   1.12500000e+00,  -3.74421937e-09,
```

Figure A.21 The Final Estimated Parameters

Finally, the output of the simulation will waveform will also be produced as below:

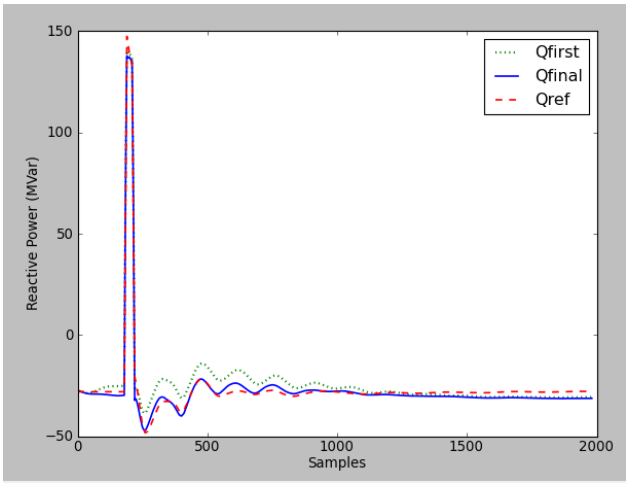

Figure A.22 The Simulation Output

REFERENCES

[1] Donald R. Volzka, Melvin I. Olken Hans B. Puttgen, "Restructuring and Reregulation of the U.S. Electric Utility Industry," *IEEE Power Engineering Review*, vol. 21, no. 2, pp. 8-10, 2001.

[2] P.L. Dandeno, R.L. Hauth, and R.P. Schulz, "Effects of Synchronous Machine Modeling in Large Scale System Studies," *Power Apparatus and Systems, IEEE Transactions on* , vol. PAS-92 , no. 2, pp. 574 - 582 , March 1973.

[3] D.N. Kosterev, C.W. Taylor, and W.A. Mittelstadt, "Model validation for the August 10, 1996 WSCC system outage," *Power Systems, IEEE Transactions on* , vol. 14, no. 3, pp. 967 - 979, Aug 1999.

[4] B. Agrawal and D. Kosterev, "Model Validation Studies for a Disturbance Event That Occurred on June 14 2004 in the Western Interconnection," in *Power Engineering Society General Meeting, 2007. IEEE* , Tampa, FL, 24-28 June 2007.

[5] Y. del Valle, G.K. Venayagamoorthy, S. Mohagheghi, J.-C. Hernandez, and R.G. Harley, "Particle Swarm Optimization: Basic Concepts, Variants and Applications in Power Systems," *Evolutionary Computation, IEEE Transactions on*, vol. 12 , Issue:2, p. 171, April 2008.

[6] Chuan-Shen Liu et al., "Identification of exciter constants using a coherence function based weighted least squares approach ," *Energy Conversion, IEEE Transactions on*, vol. 8, no. 3, pp. 460 - 467 , Sep 1993.

[7] M. Rasouli and M. Karrari, "Nonlinear identification of a brushless excitation system via field tests ," *Energy Conversion, IEEE Transactions on* , vol. 19, no. 4, pp. 733 - 740 , Dec. 2004.

[8] Tzong-yih Guo, Chuan-Shen Liu, Yung-Tien Chen, Chung-Kuang Ko, and Chiang-Tsung Huang, "Identification of model parameters of excitation system and power system stabilizer of Mingtan#6 via finalization field tests ," *Power Systems, IEEE Transactions on* , vol. 10, no. 2, pp. 795 - 802 , May 1995.

[9] L. Hajagos et al., "Guidelines for Generator Stability Model Validation Testing," in *Power Engineering Society General Meeting, 2007. IEEE* , Tampa, FL , 24-28 June 2007 , pp. 1 - 16.

[10] Jin-Cheng Wang et al., "Identification of excitation system models based on on-line digital measurements," *Power Systems, IEEE Transactions on* , vol. 10, no. 3, pp. 1286-1293, Aug 1995.

[11] E.P.T. Cari, L.F.C. Alberto, and N.G. Bretas, "A new methodology for parameter estimation of synchronous generator from disturbance measurements," in *Power and Energy Society General Meeting - Conversion and Delivery of Electrical Energy in the 21st Century, 2008 IEEE* , Pittsburgh, PA , 20-24 July 2008 , pp. 1 - 7.

[12] H.B. Karayaka, A. Keyhani, G.T. Heydt, B.L. Agrawal, and D.A. Selin, "Synchronous generator model identification and parameter estimation from operating data ," *Energy Conversion, IEEE Transactions on* , vol. 18, no. 1, pp. 121 - 126 , Mar 2003.

[13] Yunzhi Cheng, Wei-Jen Lee, Shun-Hsien Huang, and John Adams, "A hybrid method for

the dynamic parameter identification of generators via on-line measurements," in *Industrial and Commercial Power Systems Technical Conference (I&CPS), 2010 IEEE* , 9-13 May 2010.

[14] M. Ghomi, Y.N. Sarem, H.R. Kermajani, and J. Poshtan, "Synchronous generator nonlinear model identification using wiener-neural model," *Universities Power Engineering Conference, 2007. UPEC 2007. 42nd International* , pp. 236 - 241 , 4-6 Sept. 2007.

[15] R.D. Fard, M. Karrari, and O.P. Malik, "Synchronous generator model identification for control application using volterra series," *Energy Conversion, IEEE Transactions on*, vol. 20, no. 4, pp. 852 - 858, Dec. 2005.

[16] Xusheng Wu and Youping Fan, "Synchronous generator model identification using half-complex wavelet nonlinear ARX network ," *Electrical Machines and Systems, 2008. ICEMS 2008. International Conference on* , pp. 20 - 25 , 17-20 Oct. 2008.

[17] Jung-Wook Park, G.K. Venayagamoorthy, and R.G. Harley, "MLP/RBF neural-networks-based online global model identification of synchronous generator," *Industrial Electronics, IEEE Transactions on* , vol. 52, no. 6, pp. 1685 - 1695 , Dec. 2005.

[18] H.B. Keyhani, A. Agrawal, B. Selin, D. Heydt, G.T. Karayaka, "Methodology development for estimation of armature circuit and field winding parameters of large utility generators," *Energy Conversion, IEEE Transactions on* , vol. 14, no. 4, pp. 901 - 908 , Dec 1999.

[19] J. Ma et al., "Wide area measurements-based model validation and its application," *Generation, Transmission & Distribution, IET*, pp. 906-915, November 2008.

[20] Zhenyu Huang, Bo Yang, and D. Kosterev, "Benchmarking of planning models using recorded dynamics ," in *Power Systems Conference and Exposition, 2009. PSCE '09. IEEE/PES* , Seattle, WA, 15-18 March 2009.

[21] North American SynchroPhasor Initiative. [Online]. http://www.naspi.org/

[22] J. Dagle, "North American SynchroPhasor Initiative - An Update of Progress," in *System Sciences (HICSS), 2011 44th Hawaii International Conference on* , 4-7 Jan. 2011 , pp. 1 - 4.

[23] D. Kosterev, "Hydro turbine-governor model validation in pacific northwest," *Power Systems, IEEE Transactions on* , vol. 19, no. 2, pp. 1144 - 1149 , May 2004.

[24] Zhenyu Huang, M. Kosterev, R. Guttromson, and T. Nguyen, "Model validation with hybrid dynamic simulation," in *Power Engineering Society General Meeting, 2006. IEEE* , 16 October 2006.

[25] L.Y. Taylor, "Update on development of NERC requirements for verification of generator dynamic models ," in *Power & Energy Society General Meeting, 2009. PES '09. IEEE* , 2009, pp. 1-7.

[26] U.S.-Canada Power System Outage Task Force. (2004, April) Final Report on the August 14, 2003 Blackout in the United States and Canada. [Online]. http://www.nerc.com/filez/blackout.html

[27] Verification of Models and Data for Generator Excitation System Functions. (2006) NERC Std. MOD-026-1. [Online]. http://www.nerc.com/filez/standards/Reliability_Standards_Under_Development.html

[28] Verification of Generator Unit Frequency Response. (2006) NERC Std. MOD-027-1. [Online]. http://www.nerc.com/filez/standards/Reliability_Standards_Under_Development.html

[29] Define Regional Disturbance Monitoring and Reporting Requirements. (2006, Aug.) PRC-002, NERC Standards. [Online]. http://www.nerc.com/page.php?cid=2|20

[30] L.T.G. Lima, "Dynamic model validation for compliance with NERC standards ," in *Power & Energy Society General Meeting, 2009. PES '09. IEEE* , Calgary, AB , 26-30 July 2009.

[31] Z. Huang, R.T. Guttromson, and J.F. Hauer, "Large-scale hybrid dynamic simulation employing field measurements," in *Power Engineering Society General Meeting, 2004. IEEE* , Denver, CO , June 2004.

[32] I.A. Hiskens and M.A. Pai, "Trajectory sensitivity analysis of hybrid systems," *Circuits and Systems I: Fundamental Theory and Applications, IEEE Transactions on* , vol. 47, no. 2, pp. 204-220, Feb 2000.

[33] I.A. Hiskens and M.A. Pai, "Power system applications of trajectory sensitivities," in *Power Engineering Society Winter Meeting, 2002. IEEE* , 2002.

[34] I.A. Hiskens, "Nonlinear dynamic model evaluation from disturbance measurements," *Power Systems, IEEE Transactions on* , vol. 16, no. 4, pp. 702-710, Nov 2001.

[35] Ole Østerby Mary C. Hill, "Determining Extreme Parameter Correlation in Ground Water Models," *Ground Water*, vol. 41, no. 4, pp. 420-430, July 2003.

[36] Gene H. Golub and Charles F. Van Loan, *Matrix Computations*, 3rd ed. Baltimore, Maryland: Johns Hopkins University Press, 1996.

[37] ENGELBRECHT Andries P, *Fundamentals of computational swarm intelligence*. South Africa: Jon Wiley & Sons, Ltd, 11-2005.

[38] James C. Spall. (2001, March) simultaneous perturbation stochastic approximation. [Online]. http://www.jhuapl.edu/spsa/index.html

[39] J. C. Spall, *Introduction to Stochastic Search and Optimization: Estimation, Simulation, and Control*. Hoboken, NJ: Wiley, 2003.

[40] James C. Spall Xun Zhu, "A modified second-order SPSA optimization algorithm for finite samples," *International Journal of Adaptive Control and Signal Processing*, vol. 16, no. 5, pp. 397-409, May 2002.

[41] J.C. Spall, "Multivariate stochastic approximation using a simultaneous perturbation gradient approximation ," *Automatic Control, IEEE Transactions on* , vol. 37, no. 3, pp. 332 - 341 , Mar 1992.

[42] James C Spall, "Implementation of the Simultations Perturbation Algorithem for Stochastic Optimization," *Aerospace and Electronic Systems, IEEE Transactions on* , vol. 34, no. 3, pp. 817 - 823 , Jul 1998.

[43] J.C. Spall, "Feedback and Weighting Mechanisms for Improving Jacobian Estimates in the Adaptive Simultaneous Perturbation Algorithm," *Automatic Control, IEEE Transactions on* , vol. 54, no. 6, pp. 1216 - 1229 , June 2009.

[44] J.C. Spall, "Adaptive stochastic approximation by the simultaneous perturbation method ," *Appl. Phys. Lab., Johns Hopkins Univ., Laurel, MD, USA* , vol. 45, no. 10, pp. 1839 - 1853 , Oct. 2000.

[45] Quanfu Fan and Suresh Venkatasubramanian Alon Efrat, "Curve Matching, Time Warping, and Light Fields: New Algorithms for Computing Similarity between Curves ," *Journal of Mathematical Imaging and Vision* , vol. 27, no. 3, pp. 203-216, Nov 2006.

[46] Margarita Reyes-sierra, "Multi-Objective particle swarm optimizers: A survey of the state-of-the-art," *INTERNATIONAL JOURNAL OF COMPUTATIONAL INTELLIGENCE*

RESEARCH, vol. 2, no. 3, pp. 287--308, 2006.

[47] Parallel Python. [Online]. http://www.parallelpython.com/

[48] F. van den Bergh, "Effects of Swarm Size on Cooperative Particle Swarm Optimisers," in *the genetic and evolutionary computation conference* , 2001, pp. 892-899.

[49] International Energy Agency's Energy Technology Policy Division, "Technology Roadmaps Smart grids," 2011.

[50] J. Rose and I.A. Hiskens, "Estimating wind turbine parameters and quantifying their effects on dynamic behavior," in *Power and Energy Society General Meeting - Conversion and Delivery of Electrical Energy in the 21st Century, 2008 IEEE* , Pittsburgh, PA , 20-24 July 2008.

[51] Gerald T. Heydt, Vijay Vittal, Garng Huang, "Estimation of Synchronous Generator Parameters from On-line Measurements," Power Systems Engineering Research Center, Final Project Report PSERC Publication 05-36, June 2005.

[52] J. C. Spall, "An Overview of the Simultaneous Perturbation Method for Efficient Optimization," *Johns Hopkins APL Technical Digest*, vol. 19, pp. 482-492, 1998.

[53] Energy and Natural Resources Committee, "Energy Independence and Security Act of 2007,".

BIOGRAPHICAL INFORMATION

Chin-Chu Tsai was born in 1976 in Kaohsiung Taiwan, R.O.C. He received M.S. degrees in electrical engineering from National Taiwan University, Taipei, Taiwan in 2002. He has two previous work experiences. In 2002, he was a R&D engineer in charge to design USB main controller in south-bridge chip at Silicon Integrated Systems Corp., Hsinchu, Taiwan, R.O.C.. The other one is since 2003, he worked at Taipower Company, Taipei, Taiwan, R.O.C., who sponsored him to pursue his Ph.D. degree at the first two years. In 2009, He comes to Energy Systems Research Center (ESRC) at University of Texas at Arlington to pursue Ph. D. degree in Electrical Engineering. His research interests included power system stability and control, system identification, Power Market and System operation. He is a Registered Professional Engineer in Taiwan.